ΠΑΝΕΠΙΣΤΗΜΙΟ ΠΕΙΡΑΙΩΣ

UNIVERSITY OF PIRAEUS

Department of International and European Studies
MSc in Energy: Strategy, Law and Economics

THESIS

"Forecasting the fuel consumption on passenger vessels"

Author: Vasiliki Marianna Sourtzi
(Student ID nr.: MEN 17049)

Supervisor: Prof. Athanasios Dagoumas

March 2019

Dedicated to my mother
Eleni Sourtzi

Abstract

The purpose of this thesis is to develop a prediction model for fuel consumption by taking into account design, operational and environmental parameters of a typical passenger vessel (Ro/Pax type). More precisely, an ANN predictive model was developed based on 322 historical voyage reports of a typical vessel, elaborating different input variables for the development of the model. After testing 90 ANN models of varying architectures, topologies and combinations of input variables, it was concluded that a Multilayered Feed-Forward neural network model (ML FFNN) with 10-15-1NN structure is the optimal neural network, which can accurately predict the fuel consumption of the reference vessel. The findings also revealed that the model's highest prediction accuracy was achieved when exogenous factors were used as input variables, indicating that the prediction of fuel consumption is more related to exogenous variables rather than on its previous values, namely autoregressive model.

In addition to the above, the performance of the ANN model is compared with a Multiple Regression (MR), and it is observed that the former model seems to have a better forecasting accuracy as its MAPE (2.16%) is lower than the MR's MAPE (2.54%), denoting also the non-linear relationship between the fuel consumption and the input variables.

The proposed FFNN model can be integrated into the energy management system of companies with similar vessels, as it can help ship operators in choosing the most efficient measures in order not only to achieve vessel's fuel efficiency and sustained operational performance but also to reduce ship-generated emissions, fact that will also lead to lower operational costs for the shipping company. The contribution of the thesis in the literature is the provision of a more accurate method for the prediction of the fuel consumption of this vessel type through the incorporation of several exogenous variables important for the vessel operation.

Acknowledgments

First of all, I would like to express my gratitude and indebtedness to the supervisor of this Thesis, Professor Athanasios Dagoumas for his vital support, constructive feedback and motivation throughout the course of this research. The completion of this thesis would not have been possible without his academic guidance, invaluable criticism and persistent help. As my professor and supervisor, he has shown me by his example, what a good scientist should be.

I would like also to express my deepest appreciation to the rest of my Thesis committee members, Professor John Paravantis and Professor Spyros Roukanas for serving as my committee members and providing me both personal and academic guidance in order to make me a better scholar during the Master's Degree.

I am also deeply thankful to Dr. Ioannis Panapakidis for his assistance and valuable contribution in the development of the Artificial Neural Networks.

Furthermore, I would like to extend my sincere thanks to the Shipping Company, which provided me with all the necessary data and information in order the present research to be conducted. However, the Company's name cannot be disclosed but I would like to express my gratitude to all those who directly or indirectly helped me to complete this Thesis.

I owe my utmost gratitude to my family members, friends and to all those who supported me both emotionally and morally.

Last but not least, this Thesis is dedicated to my supportive mother, Eleni. Without her encouragement and never-ending love, I could not have written this Thesis.

Table of Contents

List of Figures

List of Tables

List of Abbreviations

Abbreviations	**Explanation**
ANN	Artificial Neural Network
BDN	Bunker Delivery Note
BHP	Brake Horsepower
B.N.	Beaufort Number
CFD	Computational Fluid Dynamics
CO_2	Carbon Dioxide
DBN	Deep Belief Network
DHP	Delivered horsepower
DWT	Deadweight (measurement of ship's total capacity)
ECA	Emission Control Areas
EEDI	Energy Efficiency Design Index
EEOI	Energy Efficiency Operational Indicator
EHP	Effective Horsepower
EMEP	European Monitoring and Evaluation Programme
EMSA	European Maritime Safety Agency
ETS	Emissions Trading Scheme
FC	Fuel Consumption
FFNN	Feed-Forward Neural Networks
GHG	Greenhouse Gas
GT	Gross Tonnage (measurement of a ship's internal volume)
HFO	Heavy Fuel Oil
HSFO	Heavy Sulfur fuel Oil
ICCT	International Council on Clean Transportation
IMO	International Maritime Organization
IPCC	Intergovernmental Panel on Climate Change
ITTC	International Towing Tank Conference
LM	Levenberg-Marquardt
LSFO	Low Sulphur Fuel Oil
MAPE	Mean Absolute Percentage Error
MARPOL	International Convention for the Prevention of Pollution from ships
MCR	Engine's Maximum Continuous Rate
MDO	Marine Diesel Oil
MGO	Marine Gas Oil
ML	Multilayer
MR	Multiple Linear Regression
MRV	Monitoring, Reporting, Verifying
MSE	Mean Squared Error

MT	Metric Tons (equal to 1000 kg)
NECA	Nitrogen Oxide Emission Control Areas
NO_x	Nitrogen Oxides
OECD	Organization for Economic Co-operation and Development
Pax	Passengers
R^2	Coefficient of Determination
RBF	Radial basis function networks
RNN	Recurrent Neural Networks
RO/PAX	Roll on/Roll off passenger vessel
RPM	Engine's Revolution Per Minute
S_e	Standard Error
SECA	Sulfur Emission Control Area
SEEMP	Ship Energy Efficiency Management Plan
SFOC	Specific Fuel Oil Consumption
SHP	Shaft horsepower
SO_x	Sulphur Oxides
THP	Thrust horsepower
VIF	Variation Inflation Factor

1. Introduction

During the past years it has been observed that due to the high demand of transporting goods via sea, there was a need of expanding the world's fleet. Of course, that automatically meant that at the same time the average fuel consumption has rapidly risen. Unfortunately, this fact has significantly affected the fuel prices that have been roughly increased. Despite, such increase in the fuel prices was not enough to affect the afore-mentioned trend. This is partly justifiable taking into consideration that due to globalization and the expansion of the fleet, there was also an increase in the income of the shipping companies. As the time went by, both the society and the shipping community started to deeply concern about the increase of the emissions that were produced as a result of the commercial shipping.

The beginning of this concern was the "Kyoto Protocol" which introduced a series of measures that had to be urgently adopted in order to reduce the emissions of CO_2 and therefore restrict the global development of the greenhouse gases. It was only in 2008 when shipping was included in the target of reducing the emissions of CO_2 as well as other greenhouse gases. As there was an expectation of an extreme growth of CO_2 in the future, shipping could no more be a member of a non-regulation team in this matter. Further to the "Kyoto Protocol", the E.U- MRV Regulation has been enforced in the shipping sector, suggesting that all the shipping companies and operators are obliged to monitor, report and verify the ships' emissions and consequently to observe their daily fuel consumption. At this point, it should be mentioned that most of the existing regulations are focused on the reduction of CO_2 as it is the one constituting the greenhouse gases' dominant. Also, the vessel's fuel consumption in conjunction with the ship-generated emissions is subject, which has been analyzed, taken into account various types of vessels.

According to International Maritime Organization (IMO), the vessels that produce the higher emissions are those, which are the most fuel consuming (IMO, 2018). Despite the fact that they do not represent a big part of the global fleet, the container ships and the passenger vessels, are the two most fuel consuming categories. This has been repeatedly justified by their speed and the time they both need to stay at the port area.

This research will focus on the fuel consumption of the passenger vessels (Ro/Pax), taking as a case study a typical vessel. This category has been chosen as it significantly rises

the average port emissions, which of course might not significantly contribute to the national emissions' inventory, but they are extremely important for the port's greater area and thus for the health of the crew and local inhabitants (Tzanatos, 2011). It has been proven by previous examinations that the port emissions, which are generated by seagoing vessels, can directly affect the human health. Here, it should be pointed out that this might be a result arising from the fact that port emissions, contrary to voyage emissions, can be much easily quantified.

1.1 The Research Problem

This study's first part of the research problem is to predict the fuel consumption of a typical passenger vessel, for the day ahead (next voyage) and not for the long-term future. This will be carried out by taking into account several design, operational and environmental factors which will be presented in following chapters. Further to the above, the common relationship of the fuel consumption with these variables will be examined. Moreover, the linear and non-linear methods for the prediction will be compared, while at the end the most accurate prediction method with the lower error will be proposed.

1.2 The Research Aim

To begin, one of the aims of this study is to present the variables on which the fuel consumption is depended. Then by analyzing several models, the aim is to conclude to the most accurate predictive model. It is also taken into consideration that due to the fact that the voyage of a passenger vessel is predefined regarding the distance and the duration, by optimizing various parameters, the decrease in fuel consumption can be achieved.

Additionally, another aim is to prove that by predicting the fuel consumption through the employment of ANN (Artificial Neural Network) model based on various operational conditions can lead to the proper voyage design, when several parameters and past data are known. Last but not least, another target of this paper is to show that such model can be used on board the vessel, through a real voyage and in real time conditions. Furthermore, another purpose of this study is to fill the gap in the literature review as limited studies have addressed this specific subject.

This topic is considered to be a feasible one, as there are various previous studies examining that. Moreover, any variable needed to carry out the research has been available by certified sources and thus it is considered that this study concludes to accurate evaluations.

1.3 The Research Objectives

One of this research's objectives is to cover the topic from each single perspective by analytically presenting the results of similar past studies as well as any related topics. Moreover, another objective is that the research will be conducted by taking into account only actual data and not physics models. In addition to the above, through the analysis of various models there is a short discussion on previous findings while through this study's analysis there is also an approval or disapproval of them. The research will conclude by proposing the most accurate model with the lower error, which can be used in order to predict the fuel consumption of a passenger vessel.

1.4 Structure of the Thesis

The remainder of this thesis is organized as follows. The Chapter 2 includes all the literature review concerning the International and European legislative framework focused on the ship-generated emissions and how the regulations affect the vessel's operations and consequently the fuel consumption. Moreover, all relevant studies and researches concerning the factors that affect the fuel consumption and the methods used in order to predict the bunker usage are also outlined. Further to the above, in the Chapter 3, the Artificial Neural Network (ANN), a Vessel case study and a Multiple Regression Analysis (MR) constitute the proposed Methodology. Chapter 4 includes the Data Analysis and more precisely, a correlation analysis of the factors affecting the fuel consumption, the development of the proposed ANN model, the implementation of the Multiple Regression (MR) model and a comparison between those two models. The outcomes and a summary of these methods in conjunction with a proposal for further research are provided in the Chapter 5.

1.5 The Research Questions

- Which variables have the highest impact on the fuel consumption?
- Through which model can the fuel consumption be most accurately predicted? Through a linear or a non-linear one?
- Can the Artificial Neural Network (ANN) accurately predict the fuel consumption?

2. Literature Review

In this chapter, as a more comprehensive view should be provided to the reader, some general points that are strictly connected to the examined subject, had to be presented. The target is to present a literature review which covers the topic from any aspect that might be either directly or indirectly related to it and not to be only limited in providing the results of previous findings. This is very crucial in order to underline the need of further examining this topic.

2.1 Shipping Sector and Emissions

Through the years, several studies have been focused on the development of sustainable transport. The sustainability of transport is clearly set out by the OECD (1996) and it is referred as a transport, which does not imperil the public health and has low impact to the environment. This sustainable transportation incorporates legislation, policies, systems and technologies (Global Development Research Center, 2018). Numerous guidelines, regulations and systems have been developed promoting sustainable transportation through energy efficiency measures. Hence, sustainability is considered one of the major challenges and opportunities that the maritime industry should deal, as shipping companies should change the business as usual.

Shipping industry plays vital role to the economic development and it is recognized not only as the cornerstone of the world trade as *"over 90% of the world's trade is carried by sea"* but also as a low cost transportation mean (IMO, 2018). However, the growing demand of goods will lead to a rise of the world fleet fact that will result not only to an increase in global emissions from seaborne transportation but also more fossil fuel will be required for ships' operations (Nwaoha, Ombor, and Okwu, 2016). It is well known that shipping related activities are mainly relied on fossil fuel consumption, fact that has great impact not only to the environment but also to the public health (Castells Sanabra, Usabiaga Santamaría and Martínez De Osés, 2013). This fossil fuel utilization leads to the production of greenhouse gases (CO_2) but also Nitrogen oxides (NO_x) and Sulfur oxides (SO_x), which are related to human fatalities and environmental degradation (Marine Insight, 2017). According to International Council on Clean Transportation (ICCT) (2007), for the period 1990-2007 it is

observed that seaborne emissions are increased from 585 to 1096 million tons. Moreover, Tzanatos (2011) in his research stated that, in 2008 the emissions generated from shipping amounted for 7.4 million tons and their externalities were estimated at about 2.95 billion euros.

Further to the above, despite the fact that the maritime sector is considered relatively "clean" compared to other industries as shipping emissions represent the 3.3% of the global anthropogenic emissions, this percentage is expected to be risen by 2050 (Tzannatos and Stournaras, 2014). The following chart presents (Figure 1) the CO_2 emissions from the shipping sector compared to other industries and it is observed that the maritime sector is the second largest emitter of carbon dioxide compared to other transportation means.

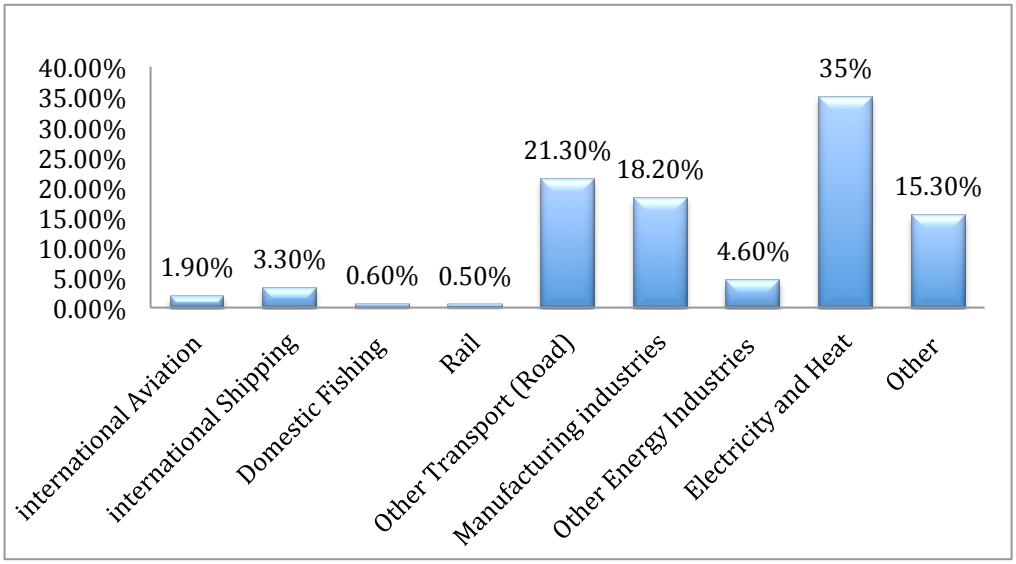

Figure 1: C02 emissions per Industry (IMO, 2019)

From another point of view, it should be stated that bunkers have always been a key factor of ships operations, as the fossil fuels account for 50%-60% of a company's operational running costs (Talley, 2012). Thus, a potential rise in the price of oil will constitute a liability, affecting negatively the profitability of the shipping company. Therefore, the need for the development of a prediction tool for fuel consumption is clearly noted as it would be considered not only as a competitive advantage but also it can attribute to the increase of company's revenues through sustained energy savings (Nwaoha, Ombor, and Okwu, 2016).

This prediction tool can be used for achieving both optimization of ship's operations and fuel efficiency (Nwaoha, Ombor, and Okwu, 2016).

In the existing literature, numerous researches have been carried out focusing on emissions estimation taking into account several variables such as transported cargo volumes, vessels itineraries etc. (Gusti and Semin, 2016). Nevertheless, the calculation of emissions is mainly related to engine propulsion, fuel type and an emission factor. The latter is determined by the characteristics, and the quality of fuel used (Gusti and Semin, 2016). Pitana et al. (2010) concluded that the emission rate could be calculated by taking into consideration the fuel consumption and the emission factor and it is given by the following equation:

$$\boldsymbol{E = FC \times EF\ ,} \tag{2.1}$$

where:

$E = Total\ Emissions\ (kg)$
$FC = Fuel\ Consumption\ (^{tons}/_{hrs})$
$EF = Emission\ Factor\ (^{kg}/_{tons\ of\ fuel})$

Another aspect that it should be pointed out here is that NO_x emissions are not tightly related to fuel usage (Aulinger et al., 2016). On the contrary, SO_x emissions are strongly dependent both on the fuel consumption and the sulfur content of the fuel used, whilst CO_2 emissions are clearly related not only to fuel consumption but also to operational conditions (Aulinger et al., 2016).

2.2 Legislative Framework

The global environmental organizations and maritime regulatory bodies have been awakened regarding the increase of atmospheric emissions generated by the shipping sector, as there was a prediction that CO_2 would be increased up to 2050 by 150% to 250% if no actions and strict measures were taken (IMO, 2009). The aforementioned results are established by the OECD (2010) too. Moreover, according to the research of IPCC (2007), the indices of the greenhouse gas emissions have been completely against the expected global reductions. However, maritime transport was considered as the least-regulated sector regarding the anthropogenic emissions, fact that led to the development and implementation of maritime policies and regulations regarding measures and actions that must be taken in order to stay within safe emission limits and to prevent the rapid deterioration of the environment

(Aksoyoglu, Prévôt and Baltensperger, 2015). Below, the existing legislations in regards of the maritime emissions are presented, divided in two main categories; the International Regulations and the European Regulations.

2.2.1 International Regulations

Until a few years ago, shipping was not deeply committed to the establishment of the Kyoto Protocol. By examining the high indices of the maritime emissions, all countries of Annex I have been requested to limit or ideally eliminate the greenhouse gases emitted by the seagoing ships, via the IMO (Lindstad H., Asbjornslett B.E. & Stromman A.H., 2011). Regretfully, that was a non-fertile measure and its results were insignificant (Lindstad H. et al, 2011). The above could be justified taking into consideration the differences in terms of the views between the Annex I and non-Annex I countries, the interpretation of Article 2.2 and the IMO's non-discriminatory regulation concerning the adoption of a common policy for all vessels trading globally (Faber et al, 2009). Upon this, the IMO focused on finding the way to reduce ships' emissions at the highest possible percentage (Lindstad H. et al, 2011). Another IMO's study provides that the efficiency of the existing global fleet can be increased from 25% to 75% through the adoption and the implementation of both operational and technical measures (IMO, 2018).

This legislative framework has been established both at international and European level in order to set standards not only for exhaust emissions but also for fuel consumption. The majority of abatement measures proposed for emissions reduction result also to the fuel consumption reduction. At this point it is noteworthy to state, that ship generated air pollutants are clearly related to fuel use.

To begin, IMO (2018) and its treaty MARPOL in the Annex VI adopted regulations aiming to limit GHG emissions and promoting energy efficiency through the efficient management of fuel consumption. More precisely, IMO's focal point lies upon SO_x and NO_x air pollutants and provide mandatory requirements in order to reduce ship-generated emissions by at least 50% from 2008 levels by 2050 (IMO, 2018). These requirements are applying to companies operating vessels above 5,000GT (gross tonnage), representing the three quarters of the global tonnage (Green, 2018). Companies should collect information and data regarding fuel use and fuel type, which will be used on future decisions in case that additional control measures, should be enforced (IMO, 2018). Further to the above, OECD (2018) states that the

decarbonization of the shipping sector will be achieved through the deployment of new technologies, new sustainable fuels and renewable energy systems.

In conjunction to all before stated, IMO developed the Energy Efficiency Index (EEDI) and the Energy Efficiency Operational Indicator (EEOI) (IMO,2018). The former sets technical standards in order to increase energy efficiency and to reduce CO_2 emissions in newbuilding vessels through the implementation of new technologies while the latter provides guidelines in order to improve both energy and fuel efficiency in the existing fleet (Hagemeister and Holmegaard Kristensen, 2011). Both energy and fuel efficiency are related to ship generated emissions and consequently to fuel consumption. More precisely, EEOI provides guidelines to shipowners and operators in order to calculate and improve vessel's energy efficiency (IMO, 2018). Such will be achieved through the procedures for designing the optimum voyage, hull's and propulsion system proper maintenance and the employment of technical measures such as the ballast water treatment and waste heat recovery systems (IMO, 2018). At this point it should be stated, that the voyage EEOI is expressed as a function of fuel consumption, CO_2 emissions, the cargo carried and the distance and it is provided by the following equation (Acomi and Acomi, 2014):

$$\boldsymbol{EEOI} = \frac{\sum_j \boldsymbol{FC_j} \times \boldsymbol{C_{Fj}}}{\boldsymbol{m_{cargo}} \times \boldsymbol{D_i}}, \quad \textbf{(2.2)}$$

where: j is the fuel type, i is the voyage number, FC_j is the fuel consumption of the fuel type j, C_{Fj} is the fuel mass of CO_2 , m_{cargo} the mass of cargo carried and D_i is the distance of the voyage i (Acomi and Acomi, 2014)

Furthermore, IMO introduced in 2016 the SEEMP (Ship Energy Efficiency Management Plan), which is considered as an operational mechanism in order the operator to monitor the performance of the vessel during the voyage and manage the energy consumption. SEEMP is a mandatory measure and it must be integrated into the Company's system, as all the data collected regarding the operation of the vessel should be reported to the Flag State (IMO, 2018). To be more precise, every vessel above 400GT must have on board a designated SEEMP, which could be subject to external inspections (IMO, 2018). The third party auditors will conduct audits and inspections to the ship and the company as well in order to assess the implementation of the SEEMP (IMO, 2018).

Therefore, it is understood that the IMO through the SEEMP obliges the shipowners and the operators not only to improve existing practices (i.e. weather rerouting, speed and

shaft power optimization, improved cargo handling, energy management etc.), but also to adopt new measures in order to boost vessel's energy efficiency and consequently ship-generated emissions will be reduced (IMO, 2018). Moreover, the Company is required to review and amend the existing SEEMP in accordance with IMO's guidelines and ship's current status, fact that will result to fleet's sustained operations (IMO, 2018).

Another measure that is adopted by the IMO regarding the anthropogenic emissions is the Emission Control Areas. The Annex VI of MARPOL established restrictions regarding the sulfur content of fuel oil onboard, forcing companies and operators to use bunker fuel onboard with sulfur content less than 3.5% m/m and from 2020 a new 0.5 % limit will be enforced (IMO, 2018). These Emission Control Areas (ECA) are divided into to two categories the Sulfur Emission Control Areas (SECA) and Nitrogen Oxide Emission Control Areas (NECA), where vessels must use fuel with low content in sulfur and nitrogen respectively (IMO, 2018). In these designated sea areas, the limit is set to 0.1% m/m sulfur content (Fagerholt et al., 2015).

For first time, in April 2018 the IMO adopted an *"Initial Strategy on reduction of GHG emissions from ships"* which is incorporated in the UN 2030 "*Agenda for Sustainable Development"* and it is considered as a framework for the Member States (IMO, 2018). IMO addresses the GHG emissions as a matter of urgency and provides short-term, mid-term and long-term abatement measures (IMO, 2018). More specifically, it sets targets for phasing out carbon emissions and it promotes the reduction of CO_2 emissions from shipping related activities by at least 40% by 2030 compared to 2008 levels (IMO, 2018). Besides the aforementioned, this strategy identifies also some barriers and promotes new technological advances in order to be overcome (IMO, 2018). However, it outlines the potential impact that its implementation may have to the Member States and presents measures in order to mitigate this effect.

At this point it necessary to state that, both US and China, which are the first and the second largest CO_2 emitters respectively, didn't sign their commitment to the aforementioned strategy (Green, 2018). This action can be justified by the fact that the abatement of shipping emissions leads to fewer voyages and consequently it affects the trade of goods. Therefore, this strategy may have impact to their economic growth as the shipping is tightly related to their economic development.

2.2.2 European Regulations and EU - MRV

As it concerns the European level, a similar to the IMO emission regulation have been adopted, namely, "Monitoring, Reporting, Verifying" (EU-MRV), by which the ships' emissions will be monitored, reported and verified (European Commission, 2017). The regulation has been enforced on 2016 and the period from 1st January 2018 until 31st December 2018 is considered as the first monitoring period (ICS Shipping, 2016). The scope of MRV regulation is that every company should monitor and report annually CO_2 emitted from its vessels (European Commission, 2016). This report should be in accordance with ISO14064, an international standard that provides fundamentals and specific conditions regarding the management of GHG emissions at organization level (ISO, 2018).

More precisely, every vessel above 5,000GT should comply with the regulation in conjunction with the fact that the fuel consumption during the voyages should be monitored and then recorded (European Commission, 2017). Additionally, it should be mentioned that in order this regulation to be in force at least one port of call during the voyage should be under the jurisdiction of EU's member state irrespective of the ship's registered flag (ICS Shipping, 2016).

Shipping companies are obliged to develop and implement a monitoring plan including not only the fuel consumption and CO_2 emissions but also other factors such as vessel's loading conditions and cargo carried during the specific voyage (Shortsea, 2017). The quantification of CO_2 will be obtained from the fuel use, the type of fuel, the bunkering volume, the technical and operational energy efficiency of the vessel and the fuel's emission factor (Stevens et al., 2015). The extracted reports from the monitoring plan will be submitted by the shipping companies on annual basis and they will be assessed by independent accredited verifiers (European Commission, 2018). Further to the above, through MRV, EU is collecting all the necessary information and data as it is considering to expand its Emissions Trading Scheme (ETS) in shipping sector (Stevens et al., 2015).

Through MRV regulation, shipping CO_2 emissions are integrated into the European Strategy for GHG reduction, which clearly specifies that the target for shipping sector is to reduce at least 40% of emissions from 2005 levels by 2050 (European Commission, 2018). In addition to all above, it is estimated that MRV will contribute to a 2% reduction of CO_2 emitted from vessels by the end of 2030 (European Commission, 2018). Therefore, it is

clearly understood that MRV will be not only the catalyst towards to the decarbonization of maritime transportation but also the foundation of an international emission system (Wan et al., 2018).

Moreover, it is noteworthy to present the key elements of the MRV Regulation. MRV introduces four different procedures to quantify the actual fuel consumption, which will be incorporated into the monitoring plan. To begin, the fist method, *"Bunker Delivery Note (BDN) and periodic stock takes of fuel tanks",* refers to the procedure that the company will extract data from delivery notes and it is clearly related to the quantity and the fuel type that was bunkered in the ship (Verifavia, 2018). This method also incorporates tank soundings and measurements that will be performed both at sea and during vessel's stay at port (Verifavia, 2018). The tank reading "at sea" consists of two separate measurements, the first takes place after the departure of vessel and the second one is carried out shortly prior the arrival of the vessel to the destination point (Verifavia, 2018). The fuel consumed at port is measured also twice, when the vessel is berthed at port and when it is unberthed. The fuel consumed or the fuel remaining on board should be converted from liters to metric tons taking into account the temperature and the fuel density (Verifavia, 2018).

The second procedure refers to *"Bunker fuel tank monitoring onboard"* and it is performed manually using a sounding tape or electronically through pressure sensors or mechanically through a tank indicator or level sensor (Faber et al, 2013). However, this procedure may lead to large deviations due to the fact that the tank's measurements and the actual consumption are never coincident.

"Flow meters for applicable combustion processes" is the third method where flow meters are used in order to calculate directly or indirectly the quantity of fuel consumed from emission sources (main and auxiliary engines and boilers) (Verifavia, 2018).

The last method is based on *"Direct emission measurements"* while the vessel is berthed at EU port and CO_2 exhaust emissions are measured in vessel's funnels (Verifavia, 2018). Under this method, the vessel's fuel consumption is calculated from exhaust emissions applying the fuel emission factor provided by the IMO (Verifavia, 2018).

In conjunction to MRV regulation, EU adopted also a Sulfur Directive (Directive 2012/33/EU) that imposes stricter limits compared to those provided by IMO's regulation. More precisely, this directive introduces a 0.5% m/m limit for sulfur content of bunker fuel

onboard and 1.5% limit for passenger vessels operating to or from port under the EU jurisdiction (Fagerholt et al., 2015). Berthing emissions are also featured in the regulation by imposing a 0.1% maximum sulfur limit to vessels remaining at port for more than 2hrs (Zis and Psaraftis, 2017).

In relation to above, EU also appointed European Maritime Safety Agency (EMSA) to conduct inspections through drones in order to verify the compliance of operators with the regulation and to identify gaps in the system (EMSA, 2018)

At this point it should be stated that the area under study is the Mediterranean Sea and more precisely the Adriatic Sea (Greece – Italy route). It is noteworthy to mention that according to EMEP (2018) in 2000, the ship generated air pollutants in the Mediterranean accounted for the 50% of the total emissions in the European seas (Cofala et al., 2007). As reported by the IMO (2018) this area is not designated as a SECA area and thus only the MRV regulation and the low sulfur limits are enforced in the designated sea area. The Adriatic Sea is divided into three segments regarding its navigable waters: international waters, European waters and ports (Buschmann and Nolde, 2018). Hence, three different sulfur limits are applied: 0.1% m/m at the ports, 1.5% within European waters and 3.5% within international waters (Verifavia, 2018).

2.3 Roll On/ Roll Off Passenger (Ro/Pax) Vessels and Emissions

This study is based on passenger vessels and more precisely on RO/PAX vessels, the acronym for Roll On/Roll Off passenger ships. This type of vessel is chosen as in Greece, seaborne passenger transport is not only related to country's economic development but also possesses a large share in the European market, representing the 17% of total passenger traffic in EU (IOBE, 2014). As stated above, the area understudy is the Adriatic Route and more precisely, the Patras – Igoumenitsa - Bari itinerary (Figure 2). According to Eurostat (2018), during the period 2016 - 2017, about 1,137,000 passengers chose the afore mentioned route, fact that makes it one of the busiest maritime routes in the Europe.

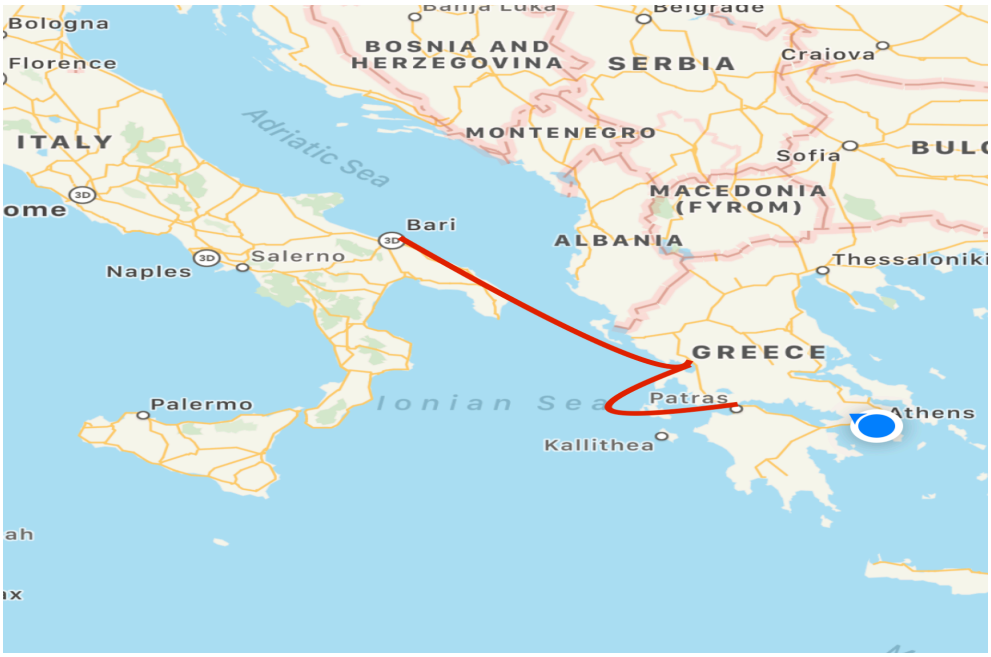

Figure 2: Map of the Adriatic Sea

Ro/Pax vessels are designed to transport both passengers and vehicles (i.e. trucks, cars etc) and their design is characterized by complexity as they combine both transportation and hotel operation services in order to accommodate passengers (i.e. restaurants, bars, cabins etc.) (Raunek, 2017). It is well known that Ro/Pax vessels have 3 ship-activities (cruising, maneuvering and hoteling) and each one of them produces a significant amount of emissions, as engine power is required to meet their energy needs (Saraçoğlu, Deniz and Kılıç, 2013) This lead to the fact, that apart from their vital role in the Greek economy another important factor that must be studied is the energy consumption in this type of vessels, as they require more power in order to meet not only the usual ship operations but also the hoteling load (Pacetti, 2012).

As far as emissions are concerned, recent researches revealed that at Greek ports anthropogenic emissions by Ro/Pax vessels account for 3.5% of the national transport GHG inventory (Tzannatos, 2010). To be more precise, at our research area, the port of Patras, the emissions generated from passenger ships contribute to more than 60% of the area's total emissions (Cesapo, 2016). Besides the aforementioned, because of the seasonality of the coastal shipping, it is observed that the impact to air quality during summer peak is higher in the designated area compared to winter months due to heavy marine traffic (Marmer and Langmann, 2005). During the summer months, passenger vessels have higher activity in the

area in order to comply with their sailing schedule, fact that leads to higher operational speed and consequently to higher fuel consumption.

In contrary to the aforesaid, companies have started to implement the practice of slow steaming not only as a measure to reduce emissions and fuel consumption but also as a way to deal with vessel overcapacity (Maloni, Paul and Gligor, 2013). However, only during the low-season (winter months), this practice is also adopted by companies owing Ro/Pax vessels. The vessels are sailing at low or eco speed in order to increase fuel efficiency and to improve fuel-related operating expenses.

2.4 Fuel Consumption

The fuel consumption is a principle exponential to the vessel's speed and it closely affects both the operational costs and the increase of GHG emissions (Meyer et al, 2012). Also, talking about fuel consumption, it should be taken into account that it is a complex variable due to its physical principles, which sometimes may lead to disputable and ambiguous results, a fact that makes a generalized explanation being virtually impossible (Meyer et al, 2012). It is necessary to state here that the vessel's total fuel consumption can be expressed as the sum of main and auxiliary engines consumptions while the vessel is at port and during its service at sea (Cullinane, 2011). In the following sections, the types of fuels and the parameters, which affect the fuel consumption, are presented.

2.4.1 Types of Fuels

To begin, an important factor that must be taken into consideration is the type of fuel oil used onboard the vessels. Several studies have concluded that the vessel's energy efficiency and the fuel consumption are related to the type of fuel used. Lundh et al., (2016) proved that variations in fuel consumption are observed during the voyages due to fuel specifications (i.e. sulfur, water, ash quality etc.). The aforementioned can also be confirmed by engines' manufactures, admitting that the type of fuel in conjunction with operational practices may result to an increment in fuel consumption (Roh and Lee, 2017).

Shipping companies and operators are forced to adopt *"switch bunkering fuel"* practice in order to meet regulations' requirements. Moreover, it should be stated that according to the international standard ISO 8217 marine fuel oils are classified into two distinct categories, the distillate and residual fuel oils. First of all, Heavy Fuel Oil (HFO) is an

industrial fuel and is also known as a "refinery residual" as it is incurred from refining process and more precisely from the distillation of crude oil (Nayak and Lakshminarayanan, 2013). As stated by Concawe (1998), HFO accounts for the 80% of the global marine fuel oils used and it is divided into three types regarding the their sulfur content. Additionally, HFO is also classified, with regard to its viscosity, to HFO 180 and HFO 380 (180 mm^2/s and 380mm^2/s) (Bomin, 2018).

On the contrary, the most commonly used distillate marine fuel oils are Marine Gas Oil (MGO) and Marine Diesel Oil (MDO) and they are both classified as low-sulfur. (Weintrit and Neuman, 2013). Their main difference lies on the fact that MGO has lower sulfur content and viscosity than MDO. It is essential to state here that these distillate fuels are more expensive but have lower sulfur content compared to HFOs (Weintrit and Neuman, 2013). Although, distillate marine fuels (MDO and MGO) have higher carbon content, fact that can be observed by their emission factors provided by the IMO (Acomi and Acomi, 2014). The table below (Table 1) depicts all the aforementioned information regarding the specifications of each fuel and their emissions factors.

Table 1: Fuel Types & Specifications & Emission Factors

Fuel Types, Specifications and Emission Factors			
Fuel Types	Sulphur Content (m/m)	Carbon Content	Emission Factors
High Sulphur Fuel Oil 180 (HSFO 180)	1% - 3,5%	≈0.85	3.114
High Sulphur Fuel Oil 380 (HSFO 380)	1% - 3,5%	≈0.86	3.116
Low Sulphur Fuel Oil 180 (LSFO 180)	< 0.5 %	≈0.86	3.151
Low Sulphur Fuel Oil 380 (LSFO 380)	< 0.5%	≈0.86	3.151
Ultra Low Sulphur Fuel Oil 180 (ULSFO 180)	< 0.1 %	≈0.86	3.151
Ultra Low Sulphur Fuel Oil 380 (ULSFO 380)	< 0.1 %	≈0.86	3.151
Marine Gas Oil (MGO)	0.1% – 1%	≈0.875	3.206
Marine Diesel Oil (MDO)	0.1% – 1.5%	≈0.875	3.206

(source: Koffi et al., 2017)

From all above, it is undelined that the "bunkering switch" process to lower sulfur content fuel oil may have impact to the profitability of a shipping company due to the fact that

low-sulfur bunkers are more expensive, resulting in additional expenses and thus an increase in freight rates will be occured (Fagerholt et al., 2015). This can also be confirmed by several studies providing that the "bunkering switch" process will increase the costs of a shipping company around 80% (Fagerholt et al., 2015). Hence, the implementation of low sulfur bunkering will affect significantly short sea-shipping companies including companies owning Ro/Pax vessels as operators will have to take a decision to either increase the ticket fare or to reduce daily itineraries (Notteboom, 2010).

Another threat that shipping companies may face is the fuel oil price volatility, in a case of a potential increase of fuel price, the cost will pass on the customer, fact that that may force the passengers to use other less expensive transportation modes, affecting negatively company's revenues (Notteboom, 2010). Moreover, another issue that must be stated is that in case that the operator chooses to use onboard the vessels low sulfur fuel oil, this decision will lead to higher CO_2 emissions due to the fact that both MDO and MGO have higher carbon content. Therefore, the fuel switching process to fuels with low sulfur content may result both on additional costs and higher carbon emissions.

2.4.2 Factors Affecting Fuel consumption and Energy Efficiency

The prediction of fuel consumption plays important role for the viability of a shipping company as already provided in previous sections of the Literature Review and it is characterized by uncertainties, as it is clearly dependent on ship's design, operational performance and environmental conditions such as the weather, hull resistance, engine specifications, fuel types etc. (Lu, Turan and Boulougouris, 2013). The actual fuel consumption is monitored onboard the vessel through mass flow meters, which measure fuel oil usage both in main and auxiliary engines right after the arrival and before the departure of the vessel from the port.

Therefore, the results of several studies in conjunction with the methodology used will be presented as several researches have been conducted through the years in order to predict both real time and future voyage fuel consumption. These studies were carried out through the employment of several predictive models or physical empirical models by combining various design, operational and environmental parameters. The findings of previous researches and the analysis will help us to choose the right variables for our predictive model.

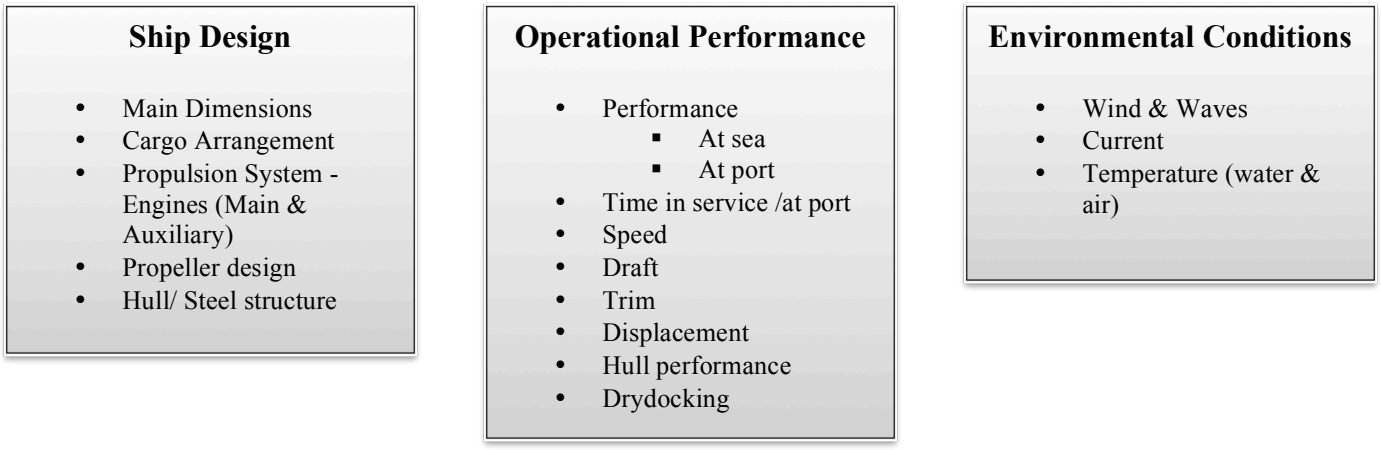

Figure 3: Factors Affecting Fuel Consumption (source: author)

Further to the above, it should be stated that this section is divided into three main subsections where the aforementioned parameters will be provided in accordance with the categories presented in the Figure 3.

2.4.2.1 Ship Design

Several attempts have been made in order to estimate and calculate the fuel consumption taking into account the ship design. Most of the researches are conducted by investigating the propulsive power, hull resistances, engines' specifications in combination with various operational and environmental factors in order to conclude to a more precise prediction of fuel consumption.

To start with, Cullicane (2011) conducted an Ordinary Least Squares (OLS) in order explore the association between the fuel consumption of containerships by taking into consideration various design variables such as the size of the vessel in combination with the installed propulsion power. From the findings, it is observed that not only the aforementioned variables have great impact on the fuel consumption but also economies of scale can be achieved by applying efficient ship design. Tezdogan et al. (2014) also focused their research on ship design and they estimated both the fuel usage and the effective horsepower by examining the vessel's total resistance through the implementation of VERES CFD (Computational Fluid Dynamics) simulations for container ships. Lu, Turan and Boulougouris (2013) used the empirical formula of Holtrop – Mennen for the estimation of vessel's total

hull resistance and they modified the Kwon semi-empirical model in order to conclude to more accurate prediction of fuel consumption by taking into account also the effect of weather conditions in the hull form.

From the above studies, it is concluded that the ship resistance is considered a crucial component for the prediction of fuel consumption (Molland, 2011). The hull's total resistance is defined as a sum of ship resistance in calm waters and the added resistances. Ship resistance in calm waters results to power losses due to fact that the ship's hull is in contact with the viscous fluid and it is divided into three other *"resistance categories":* frictional resistance, viscous pressure resistance and wave resistance (Molland, 2011) .The latter can be also divided into wave breaking and wave pattern resistance (Molland, 2011). However, the viscous pressure and wave resistance are also referred as residuary resistances of the ship (Molland, 2011). All the equations used in order to estimate the afore mentioned resistances are provided in the Appendix A section.

To begin, frictional resistance is associated to the vessel's wetted surface, speed, and hull roughness, contributing to the 40% of the total resistance of Ro/Pax vessels (Jang et al., 2014). Higher frictional resistance is also observed to ships operating in low speed (Wartsila, 2018). Thus, it is understood that a potential decrease to hull roughness and consequently to frictional resistance will lead to reduction in fuel consumption (Molland, 2011). On the contrary, viscous pressure resistance is related not only to speed but also to the wetted area and it represents about 5 – 10% of the total resistance of a Ro/Pax vessel, while the wave resistance accounts for 50 - 55% (Molland, 2011). Several empirical methods and CFD computations based on Navier – Stokes Equations (i.e. RANS, URANS etc) have been used in order to estimate and calculate vessel's resistances under different operational and environmental conditions. However, the most commonly used mathematical model was developed by Holtrop and Mennen (1982) for the empirical calculation of the total resistance based on real time conditions.

Another aspect that must be investigated is the association between ship's power system and the fuel consumption. Coraddu et al., used MATLAB's simulation tool SESAP in order to forecast and evaluate the fuel consumption through the exploration of energy system processes (i.e. main & auxiliary engine specifications, engine loads, diesel generators load etc.) operating under different conditions. More precisely, they applied the above-mentioned

Sustainability Analysis to a tanker and modeled its electrical network based on vessel's operational data.

At this point, it is noteworthy to state that Main Engines, Auxiliary Engines and Boilers, which are considered as prime movers, constitute ship's power train, while the gearbox, the shaft and the bearings are interfering between the prime movers and the propeller, transmitting mechanical energy to the propeller (Molland, 2011). The Figure 4 depicts that the ship drive train can be expressed as a function of different power outputs. These different power outputs occurred due to transmission losses in the ship's energy system as both mechanical and fluid losses took place in the gearbox, shaft and the propeller, accounting for the three-quarter of the fuel energy affecting the ship's efficiency (Molland, 2011). Therefore, it is understood that the engine's power incorporates power occurred not only from losses in the gearbox and shaft but also from the hull resistances (Molland, 2011).

This complex energy system can break down into Brake horsepower (BHP - P_B), Shaft horsepower (SHP - P_S), Delivered horsepower (DHP), Thrust horsepower (THP) and Effective horsepower (EHP) (Molland, 2011). More precisely, BHP refers to the engine's power output, which is predetermined by the engine manufacturer (Molland, 2011). The SHP is defined as the difference between the BHP and the losses occurred in the gearbox (Carlton, 2012). The reduction gearbox is a critical part in the marine transmission system as they used to reduce the engine's revolutions per minute (rpm) to lower propeller's rpm while the engine is performing in full power (Carlton, 2012).

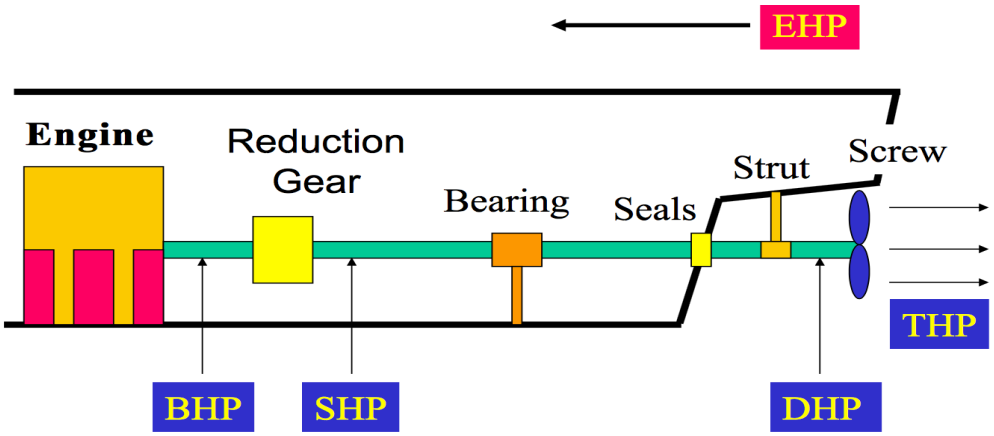

Figure 4: Ship's Drive Train (source: Castello Branco, 2011)

According to Woud and Stapersm (2002), the frictional losses in the gearbox are estimated between 3 - 5% and the gearbox efficiency η_{GB} is ranging between 0.95 and 0.97 depending on the gearbox specifications(Woud and Stapersm 2002). Afterwards, the difference between the SHP and the losses in bearings and seals form the DHP and it should be greater than the effective horsepower, the shaft efficiency of shaft η_s is estimated between 0.98 and 0.99 (Woud and Stapersm 2002). Also, it should be noted that the DHP is clearly correlated to the fuel consumption as it is observed that a potential increase in the delivered power results to an increase of the fuel usage (Woud and Stapersm 2002).

As it concerns the THP, Woud and Stapersm (2002) have concluded that it can be expressed as a subtraction between the delivered power and the propeller losses and the propeller efficiency η_P takes values between 0.65 – 0.75 when the ship is operating at design speed. From the other hand, EHP is referred to the power output in order the vessel to operate without the existence of the propeller taking into account the hull resistance in calm waters and the operating speed (Woud and Stapersm 2002). All the equations for estimating the aforementioned horsepowers are presented in the Appendix B section.

After presenting the losses occurred in the ship's drive train, another important parameter is the specific fuel consumption (SFOC) of main engine in calm waters. The SFOC of main engines is provided by the manufacturer as it is dependent on the type and the specifications of the engine installed, in conjunction with the engine load factor and the maximum continuous rating (MCR) (Roh and Lee, 2017). However, variations in the SFOC are observed during the voyages resulting also in fluctuations in the fuel consumption due to several reasons, for example the fuel specifications may cause an increase in fuel consumption (Lundh et al., 2016). From the above findings, it is denoted that the total fuel consumption can be expressed as a function of SFOC and the BHP and it is provided by the following formula:

$$\boldsymbol{FC = \int P_B\ SFOC(P_B)dt}, \quad \textbf{(2.3)}$$

where: P_B is the BHP (Brake Horsepower) and SFOC is the Specific fuel consumption.

Furthermore, an increment of 6% in fuel consumption is also noted between the time interval of the engine overhaul taking into account all parameters including also the fuel quality (Wartsila, 2018). At this point, it should be stated that MCR of the brake horsepower indicates the maximum power output in which the engine's load is generated while the speed is maintained without causing failure to the machine (Roh and Lee, 2017).

Another aspect that must be considered is the sea margin, which is playing crucial role in the speed – power relationship and consequently to fuel consumption (Kim et al., 2017). More specifically, during the ship design process the ship resistance and power output estimation in calm waters are the focal points, but also sea margin calculation is also considered necessary as it shows how the added resistance affects the power output (Kim et al., 2017). In other words, sea margin projects the increase of the required power when the vessel is operating in actual waters as it incorporates all environmental factors (added resistance, hull fouling etc.) that have impact in the performance of the vessel (Magnussen, 2017). According to Arribas (2007), the sea margin is estimated between the interval of 15% and 30% where the 10% it is occurred by the wind and waves affecting the ship's performance (Molland, 2011).

2.4.2.2 Operational Performance

To begin, Nwaoha, et. al (2016) applied successfully Fuzzy Rule Base (FRB) in conjunction with Utility Theory (UT) in order to estimate the fuel consumption of diesel engine powered vessels taking into consideration various operational parameters such as ship's hull and propeller condition, engine efficiency, routing, loading and weather conditions etc. Their study provided successful modeling results and they concluded that the engine's efficiency plays crucial role to the fuel consumption as it has been observed that the fuel use is reduced in cases when both main and auxiliary engines are operating in optimal point (Nwaoha, Ombor, and Okwu, 2016).

Papanikolaou (2014) provided that the fuel consumption is strictly related to the engine's load in combination with engine's operating hours as in case it operates continuously beyond a predefined limit may result to higher fuel consumption. The above mentioned is also proved by Borkowski, Kasyk, and Kowalak (2011) through the implementation of both a sea trial program and empirical formulas (i.e. specific fuel consumption, effective power formula etc.) in accordance with ISO standards and the employment of Least Square method (LMS) by taking into account sea trial records. To be more precise, the results of their study showed that the estimation of the fuel consumption is dependent on main engine operational state and its continuous operating time. Kee, Lau Simon and Yong Renco (2018) in their research conducted Statistical Analysis in order to predict both the fuel use and the speed curve. So,

they developed a Multiple Regression model for forecasting the fuel consumption, which included five independent variables (distance, travelled hours, vessel speed, DWT and wind). Their study was based on operational data from two tugboats. In addition to all above, they used performance curves in order to estimate the optimum speed for the lower fuel consumption.

Further to the above, Wartsila (2015), through its research program, concluded that proper maintenance of marine engines is also an important issue in order a vessel to operate efficiently and to void any decrease in power output, fact that will result to more energy usage and consequently to higher fuel consumption. Wang et al. (2017) proposed a successful LASSO (Least Absolute Shrinkage and Selection Operator) regression model in order to predict fuel consumption taking into account several operational variables depicted in the vessel's reports (i.e. speed, trim, displacement, cargo weight etc.). The results revealed that the prediction ability of the model is more accurate than a multiple regression model (MR).

Carlton (2012) in his research stated that the hull condition is also related to power and fuel consumption due to ship's frictional resistance, because the hull's fouling can increase the fuel usage by 30-40% and consequently emissions increase too. This is justified by the fact that in order the vessel to maintain its speed, additional power is required. This issue has been addressed by the EEDI (Energy Efficiency Index), promoting several methods such as anti-fouling coating and paints in order to reduce hull roughness (IMO, 2018). Furthermore, it should be noted that hull roughness is strongly related to the age of the ship, the time spent at sea and at port and the vessel's speed (Magnussen, 2017). It is apparent that ships with longest stays at ports and operating at low speed have the tendency to develop fouling (Giorgiutti et al., 2014).

According to other studies, the age of the vessel also plays crucial role to hull degradation and a 8 year vessel has hull roughness approximately 400 - 500 micrometers, which results to a 33% power increase in order the vessel to sustain its speed, fact that is also depicted in the Figure 5 (Hellio, 2009). However, according to International Regulations, passenger vessels should be out of service every two years for their maintenance, where hull cleaning and coating takes place (Hellio, 2009). After the hull cleaning, the hull degradation and consequently the resistance due to fouling are both decreased (Hellio, 2009). Molland et al. (2011) in their research concluded that the resistance margin due to hull roughness is

estimated to 10% in case that no hull maintenance is carried out during these two years where the vessel is in service. Although, passenger's vessels are less prone to marine fouling, compared to commercial vessels (i.e. tankers, bulkers etc.) due to their higher speed, and the short port stays (Hellio, 2009).

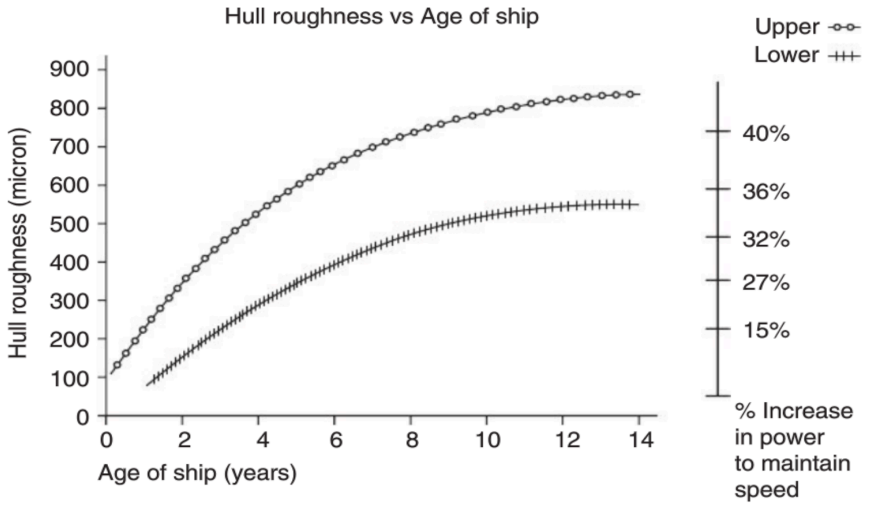

Figure 5: Hull roughness vs Age of ship (source: Hellio, 2009)

From all above, it is denoted that an increment to ship's resistance can also be occurred due to deteriorative effects to hull and the propeller (Molland, 2011). These effects are a combination of ship design and environmental factors and they are divided into hull and propeller fouling and hull and propeller roughness and all of them have direct impact to vessel's speed resulting in the rise of propulsive power and consequently to the increase in fuel consumption (Molland, 2011). The hull fouling is considered uncontrollable variable and it is difficult to be forecasted as its increase is not linear and it is related to many operational parameters (Molland, 2011). Thus, the hull's roughness can only be expressed as an increase in the ship's frictional resistance.

Another factor that affects the ship's fuel consumption is the vessel's loading conditions. Alderton (1981) built a formula that estimates the fuel consumption but without taking into account the vessel's total weight, resulting to relatively high deviation compared to actual consumption of a ship. From the other side, Coraddu, et al. (2017) applied Gray Box Models (GBM) in order to forecast the fuel consumption and they concluded that the trim optimization leads to lower fuel consumption, as it considered one of the easiest practices in

order a sustained operational performance to be achieved. Lee et al. (2014) combined White Box Numerical Models (WBM) and CFD in order to find also the optimal trim for several types of vessels. Moustafa, Yehia and Hussein (2015) used the Holtrop –Mennen's method through the employment of CFD software in order to estimate the ship resistance and they also proved that the trim optimization leads to higher fuel savings.

Variations in fuel consumption have been observed when the vessel is in ballast or partially loaded or fully loaded (Tiling et al., 2018). The loading conditions of Ro/Pax vessels vary, as their trading pattern is known right before its departure from the port and the loading plan cannot be developed in order to better accommodate the vehicles, trucks, trailers etc. achieving the optimal loading conditions. Therefore, the ship's draught differs depending on the volume of cargo loaded, fact that results to added resistance to vessel's hull and especially to bow region (Tiling et al., 2018). Additionally, as stated by Reichel et al., (2014) the employment of CFD software proved that the trim optimization of a vessel can contribute to hull resistance deduction and consequently to reduction of fuel consumption by 1%-3%. Thus, in case that this practice is applied to vessels, which are not fully loaded, the reduction in fuel usage is estimated up to 5% (Reichel et al., 2014).

It is noteworthy to state that the speed is also a dominant factor that must be investigated in relation with the fuel consumption as it plays crucial role both for the operator and the customer (Mander, 2017). During the last years, it is observed that many companies and operators change the fleet operational practice by adopting the slow steaming (decreasing the vessel's speed) in order not only to minimize the fuel cost and but also to meet International Regulations requirements concerning the fuel emissions limits (Mander, 2017). The voluntary speed reduction was introduced during 2007 by the shipowners, as response to high global oil prices (Mander, 2017). However, the reduction of the vessel speed has as an effect, the extension of the voyage time (Mander, 2017).

First of all, it should be mentioned that the relationship between the speed and the fuel consumption is non-linear and a quadratic function of speed is applied in order to estimate the vessel's bunker consumption (Fagerholt, Laporte and Norstad, 2010). Gusti and Semin (2017) developed and implemented a speed optimization model resulting that when the vessel is operating in optimum speed, the fuel consumption decreases compared to the service speed provided by the engine's manufacturer during the sea trials. Moreover, other studies presented

that the fuel consumption is strongly correlated to vessel speed in conjunction with weather conditions (Gusti, and Semin 2016). However, in Ro/Pax vessels, the speed is also affected by other factors such as port speed limits, and the speed variations during the voyage (Gusti, and Semin, 2016). Prpić-Oršić et al. (2016), used both MATLAB and FORTRAN to carry out numerical analysis and they concluded that the afore mentioned variations can be resulted either by speed reduction due to fuel economy reasons or to maintain the vessel afloat and seaworthy or by sea state conditions which is also referred as involuntary speed reduction. Moreover, the speed loss has been estimated by taking into account the engine and propeller performance indicators. More precisely, Arribas (2007) performed Linear Regression and concluded that the vessels consume 15-30% more energy when operate in actual conditions compared to the energy required when they operate in calm waters due to resistance caused by wave and wind forces. Furthermore, Wang et. al, (2013) applied Pareto- optimal solutions and they concluded that the speed optimization leads to lower fuel consumption and consequently to lower CO_2 emissions.

The relationship between the fuel consumption and the speed of containerships has also been investigated by Notteboom and Vernimmen (2009) through the employment of empirical models and the outcomes revealed that a minimum rise in vessel speed may result to an exponential increase to fuel consumption and thus the non-linear relationship between the aforementioned variables is illustrated in the Figure 6.

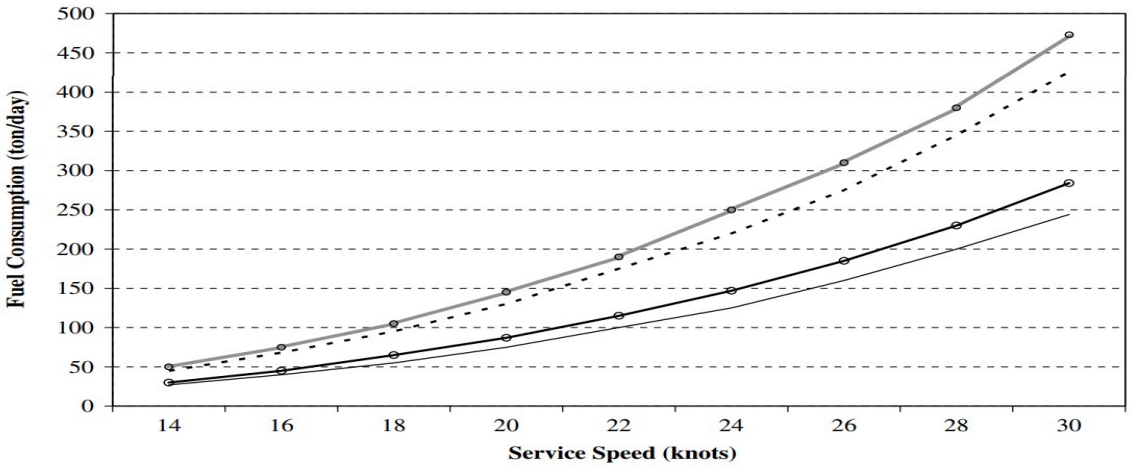

Figure 6: Fuel Consumption vs Service speed (source: Notteboom and Vernimmen, 2009)

Moreover, Coraddu et al. (2017) applied the LAR (Least Angle Regression) method in order to identify the features with greater impact on fuel consumption. The results from their research provided that the propeller pitch in conjunction with the vessel's speed are considered as the most critical variables for determining the fuel consumption as both they depict the overall operational performance of the propulsion system. Nevertheless, other studies investigated the association between the speed loss and the fuel consumption and how the former affects the latter one. More specifically, it is observed that when the ship is operating in high speed the mechanical losses increase compared to those observed when performing at low speed, resulting in a rapid rise in fuel consumption (Oleksiy et al., 2013). Banawan, Mosleh and Seediek (2013) focused on the prediction of fuel consumption in catamaran vessels by taking as variable the operational speed. Through the employment of Maxsurf program in combination with model experiments, they concluded that a potential reduction in the fuel consumption could be achieved through the speed lowering.

2.4.2.3 Environmental Conditions

Tillig et al. (2018) in their research applied uncertainty analysis in conjunction with Monte Carlo simulation and the findings revealed that the predicted fuel consumption is different from the real-time results and the accuracy of the model was estimated around to 60%-70%. This deviation can be justified due to incomplete observations and missing parameters such as *"the water depth, rudder angle and water current"* (Tillig et al.,2018). From the other hand, Bialystocki and Konovessis (2016) by applying an algorithm, concluded to a 0.81% deviation of the predicted fuel consumption from the actual calculations as they didn't take into account also the water current, sea condition and wind directions. Kim et al. (2017) by applying CFD and URANS method in both operational and environmental parameters, the results showed that the lower ship's service speed, the higher involuntary speed loss is noticed due to effects of the wind and wave and especially wave forces play important role to this observation. Furthermore, Yuan and Nian (2018) used as a reference vessel for their research, a tanker and they developed a Gaussian Process Metamodel in order not only to assess the interaction of different factors (engine, weather conditions etc.) to the vessel's fuel performance but also to predict the fuel usage under different wave and wind conditions.

It is denoted from the findings of the above-mentioned studies that the environmental conditions have significant contribution in order to get an accurate prediction for fuel consumption (Magnussen, 2017). Hence, the added resistance from wave and wind cannot be neglected as both have significant impact to ship's speed and consequently to the fuel consumption (Henk, 2006). At this point it noteworthy to state that the term "added resistance" is used in order to explain the occurrence of energy loss due to external factors and it is described as the sum of resistances due wind, wave sea's composition and current (Henk, 2006). All the afore mentioned principles constitute the Added Resistance due to environmental factors and they contribute in the increase of Total Resistance R_T of the vessel. (Magnussen, 2017).

As it concerns the added resistance due to waves, it refers to the effects of waves over the vessel's hull (Molland, 2011). The resistance of a vessel can be increased by a 15-30% when she is operating in actual conditions in comparison with calm waters and a great percentage of this increase is resulted from the added resistance due to waves (Henk, 2006). Moreover, it should be noted that the latter is strongly related to the vessel's speed and it is observed that as the speed increases, the wave resistance is escalating (Molland, 2011). The added resistance is expressed as a function of wave characteristics and the vessel's speed (Molland, 2011). Through the years several methods have been developed in order to estimate the wave resistance in actual waters. More precisely, the most commonly used method is through the combined application of both empirical models and CFD software (Molland, 2011).

The added resistance due to wind refers to the effects of the wind loading not only to the hull but also to the above-water hull. According to Molland (2011) the air resistance accounts a 4-8% of ship's total resistance. The air resistance R_{AA} is associated with the wind speed and direction as well as with the particulars of the superstructure (i.e. dimensions and shape) and the vessel's speed (Molland, 2011). The wind parameters are provided by the IMO (2012) guidelines where a Beaufort Number (B.N.) describes each sea state in accordance with the wind speed and direction and are depicted in the following table (Table 2).

Table 2: Wave characteristics corresponding to Beaufort Number

Wave Characteristics corresponding to B.N			
B.N	**$H_{1/3}$(m) - significant wave height**	**T_{01} (s) – mean wave period**	**λ (m) – wave length**
0	0.0	0	0.0
1	0.1	1.22	2.32
2	0.4	2.44	9.29
3	0.8	3.45	18.57
4	1.5	4.73	34.91
5	2.0	5.46	46.52
6	3.0	6.67	69.43
7	4.5	8.19	104.67

(source: IMO, 2012)

Another parameter, that has impact on hull resistance, is the added resistance due to seawater and consequently it affects also the fuel usage (Henk, 2006). This can be justified by the fact that the water properties are different from those of the actual water (Magnussen, 2017). More precisely, this composition can be expressed as a function of temperature, density, viscosity and salinity (NPL, 2018). Therefore, these mentioned factors should be taken into account in order to have more accurate estimation of the added resistance due to seawater. Festus and Samson (2015) applied ITTC-57 methods and their observations revealed that there is a strong association between the hull resistance and the density of the seawater. Hence, a potential increase in the density of the water causes not only an increase on hull resistance but also an increase effective power, fact that has a negative effect in vessel's fuel efficiency (Festus and Samson, 2015).

In addition to above stated, Manheim (2017) also proved that the temperature of the seawater is playing crucial role as both the viscosity and density are related to the former principle. It is necessary to state that these properties are relative to location and season and thus variations in the temperature, viscosity and density are minor (Magnussen, 2017). Therefore, in the most of the studies conducted, the additional resistance is estimated based on the typical seawater temperature ($T = 15° C$) and density $\rho = 1{,}026\ kg/m^3$, without taking into account the afore mentioned variations (Magnussen, 2017).

All the methods and the models, which are employed in order to estimate the Added Resistance due to environmental factors, are outlined analytically in the Appendix A section.

2.5 ANN for Fuel Consumption Prediction

This section focuses in presenting only the researches that applied Artificial Neural Networks (ANN) in order to predict the vessel's fuel consumption. To be more precise, the selected variables, the type of ANN used and the obtained results are outlined. It is noteworthy to state here that from the above analysis of previous studies and their findings, it is observed that there are limited researches that use the Artificial Neural Networks predictive models in order to forecast vessel's fuel consumption and her operational performance. On the contrary, ANN is widely used in numerous studies for predicting the fuel usage in various means of transportation (i.e. airplanes, trucks and vehicles).

First of all, Bal Beşikçi et al. (2016) developed an Artificial Neural Network (ANN) prediction model including seven input variables provided by noon dataset (speed, trim, draft, weather conditions, quantity of the cargo) in conjunction with engine's RPM. This ANN model was used in a latter phase so a decision support system (DSS) for energy efficiency in real time operations to be built. Furthermore, the predictive ANN model was compared to Multiple Regression (MR) model leading to the outcome that the former achieved better prediction performance than the latter.

Moreover, Weintrit and Neumann (2017) developed also an ANN and more specifically a DBN (Deep Belief Network) in order to forecast a ship's fuel consumption based on ship's operational data. They used several input variables combining both operational, design and environmental parameters (distance, load, trim, draft, vessel specifications, wind, swell, wave length) leading to a high accuracy model. The developed DBN model in combination with the weather rooting software can provide information about the variations of fuel consumption when the vessel is operating under various environmental conditions.

In addition to all above, Petersen, Winther and Jacobsen (2012) modeled the fuel consumption for real time conditions through the implementation of Tap-Delay Artificial Neural Network. More specifically, the factors that describe the dynamic state of the vessel (i.e. speed, trim, draft, propeller pitch and engine's rpm) have been collected through sensors and they were used as input variables to the model. The outcomes from this research provided that this model can obtain accurate results and it can be used for vessel's trim optimization.

From the other hand, Pedersen and Larsen (2009) presented in their study a neural network for propulsion power predicting model by taking into account, vessel's noon report dataset, weather and onboard measurement data. They concluded that the ANN model is more accurate compared to other linear and other non-linear models.

Taking into consideration all the above, it is outlined that the developed models presented in these researches were mainly based on vessel's operational data collected either by vessel's noon reports or through sensors on board.

3. Research Methodology

In this chapter, the outline of the methodology implemented will be described in order this study to be carried out and to answer the research questions. More precisely, the structure of the research is stated through the research design, the techniques for collecting the data as well their reliability and validity are also presented. Furthermore, the research approach plays crucial role in order to draw conclusions as it shapes the design and denotes possible limitations and delimitations. In addition to all above, the specifications of the vessel, which is used as a case study, are also provided in this chapter. Last but not least, Artificial Neural Network (ANN) model and a Multiple Linear Regression (MR) model will be also presented.

3.1 Research Design

To begin, this thesis was conducted by interpreting quantitative secondary data as its quantified nature is entirely obvious and the purpose of this research is exploratory, descriptive and predictive as well. This can be justified by the fact that the interaction between the input variables will be explored and described, the response of these variables under different operational conditions will be evaluated and finally the prediction of vessel's fuel consumption will be modeled.

The implementation of the afore mentioned methodology will lead to the employment of both descriptive and predictive analytics tools. A predictive Artificial Neural Network will be developed and it will be used as a model in order to address the objectives of this study. The choice of this predictive method was based on the fact that provides more accurate predictions compared to other predictive models as it is well suited in real-time data in combination with its generalization capability.

The ANN model will be built, by using previous researcher's conclusions, existing empirical models and theoretical findings that will be applied to actual condition case study in order not only to choose the most suitable combination of input variables but also to explain the performance and the outcomes of the network. In conjunction with all above, the case study approach is also interpreted, as a modest scale study will be employed by enabling the exploration and the investigation of the fuel consumption under real – time vessel's operating conditions through continuous historical observations.

In order to build an accurate prediction model, factors such as vessel's speed, main engine working hours, fuel consumption, distance, weather conditions and the weight of the vessel are taken into account. Therefore, previous theoretical and empirical findings will be applied. It is necessary to state that these factors should encompass ship design, environmental conditions and operational performance. After identifying the topology of the ANN network, the selection of the best architecture will take place and the training process will be employed in order to learn the complex associations between the input variables and the output. Furthermore, it is noteworthy to be stated that the data used will be divided in two subsets, the one set will be used to train the network and the second to test the performance of the model.

Moreover, a correlation analysis will be conducted between the fuel consumption and the selected variables in order to identify the integration among them. Apart from the ANN model, a Multiple Regression model (MR) will be also developed as well to examine also the relationship between the dependent variable and the predictor factors. The performance and the accuracy of both models will be evaluated through Mean Absolute Percentage Error (MAPE).

3.2 Data Collecting Techniques, Validity and Reliability

It is widely known that in order to feed, train and validate the ANN prediction model, a significant amount of dataset is required. This research is mainly based on the ship's operational recorded data that are depicted in voyage reports. This dataset, extracted from the MRV software, and it contains: the date, the time, the voyage number, departure and arrival ports, the vessel speed, the duration of the voyage, some hindcast weather data (B.N.), engine load, the vessel's loading conditions (cars, passengers, trailers, buses, motorcycles and trucks), the voyage total fuel consumption, the voyage consumption per engine (main and auxiliary

engines), boiler and fuel type (MGO, HFO, LSFO), vessel's draft (trim, aft, fore) and CO_2 emissions. The crew onboard feed this voyage report every 24h with all necessary data provided by the measurement instruments during the voyage and vessel's stay at port. This study was carried out by taking into account 322 electronic operational reports which are referred to the period from 1st January 2018 until 31st October 2018 for one vessel that is operating in the Adriatic route (Patras – Igoumenitsa – Bari). The research data contains one excel file provided by the Shipping Company showing all the afore mentioned dataset. Hence, the aforementioned 322 observations are considered sufficient to develop an ANN prediction model.

The theory, that deals with the vessel's fuel consumption, emissions and the design, operational and environmental factors which affect the fuel usage as well as the outcomes from previous studies and research papers regarding the models used in order to predict the fuel consumption are provided in the literature review section. The results in conjunction with the collected data from the vessel's voyage reports are demonstrated and analyzed in the Data Analysis chapter where also the development of ANN and MR predictive models will be presented.

Furthermore, despite the fact that the Company through its official website presents ship's particulars and specifications, although, some necessary information is not provided, such as the calm water resistance, hull design dimensions etc. All these factors are considered necessary data in order to have an accurate prediction of fuel consumption. Unfortunately, ship's hull parameters cannot be estimated through mathematical calculations based on empirical methods and findings from previous research papers as they are provided only from the Shipbuilding Company during the seakeeping and model tests. These data are considered sensitive and could not be officially declassified by the shipowing Company, consequently these design parameters that affect the fuel consumption couldn't be taken into account. It is important to state here, that this limitation may have impact on the model's performance, resulting in lower predictive accuracy. As a result, the focus of the research study is based more on parameters depicted by the vessel's voyage reports rather than on the design factors. In addition to all above, it is necessary to state that the Company's name as well as the name of the vessel cannot be disclosed and thus the name of the vessel used as a case study is fictional.

The dataset provided by the voyage reports outline the average values of the aforementioned data, fact that does not provide the ship's operation under real - time conditions. Another aspect that must be mentioned is that even if these reports are obtained by the company which owns the vessel, the data are filled manually by crew members leading to the fact that their validity may be doubtable as these log data may be exposed to human factor or error.

At this point, it is worth noting that it is assumed that the data gathered will be valid as the company's Operations department checks, monitors, and evaluates daily the data recorded in the voyage reports and in case that implausible data or an error occurs, the department is in a continuous communication with the ship's officers in order to correct imprecise observations and harmonize the data. Last but not least, the data regarding the ship's particulars are obtained by Company's official website and they are considered both valid and reliable.

3.3 Case Study – Vessel ROPAX-NI

In order the present study to be conducted, a Ro/Pax ship is used for a demonstrative case study. The reference ship is the Passenger/Ro-Ro ferry, M/V ROPAX-NI, which is performing a regular service in the route Patras – Igoumenitsa – Bari for more than 8 years. M/V ROPAX-NI is a high-speed vessel and it is owned by a Greek based shipping company. This ship is selected as our case study because it is operating in the chosen geographical area presented in the Literature Review section. In this thesis, the research and the analysis is mainly relied on the data set of this specific ship which incorporates all the specifications of a typical Ro/Pax. The shipwoner provided all the necessary data in order this study to be carried out for this specific vessel and the proposed ANN prediction model can be generalized also to other Ro/Pax vessels with similar particulars without changing the selected input variables of the network.

The vessel has carrying capacity of 800 passengers and 140 trucks/ 500 vehicle cars and its guaranteed service speed is up to 23 knots. More precisely, the specifications of a typical passenger ship are presented in the Table 3. The vessel is operating in the route daily and more precisely, during the low season, from October until May, the vessel departs from the port of Patras every second day at 18:00, arriving at the port of Igoumenitsa and Bari at 23:59 and 10:30 (the next day) respectively. From the port of Bari, the vessel departs at 20:30

and arrives at the port of Igoumenitsa and Patras at 05:30 and 13:00 (the next day) respectively. It should be stated that the departure and arrival times correspond in Greek local time (GMT +2). Hence, it is observed that the voyage duration is 16hr and 30min and the distance covered is approximately 318 nautical miles. During the high season, from June until September, the vessel reaches also the Corfu port departing from Igoumenitsa port but not on daily basis. The voyage duration for this specific itinerary is 9hr and 30min and the distance covered is 197 nautical miles. Moreover, it is noteworthy to mention that every two years, the vessel is out of service for a month in order to carry out its planned drydocking and annual maintenance.

Table 3: Ship's Particulars (M/V ROPAX-NI)

Ship's Particulars			
Vessel Name	ROPAX-NI	**Deadweight**	9,000
Type of vessel	RO/PAX	**Draft (m)**	6.4
Flag State	Greece	**Nr. Passengers**	800
Gross Tonnage	24,600	**Propulsion power (total KW)**	24.000
Length overall (LOA)	200	**Guaranteed Service Speed (% MCR, sea margin)**	23 knots (80% MCR, up to Beaufort)
Length BP (m)	177		

Apart from the geographical area where the ship is operating, another factor for choosing this case ship is that the EU-MRV regulation has been implemented to this specific vessel from January 2018 and the company has developed a MRV Monitoring Plan in order to record and then verify all necessary data regarding the emissions and fuel consumption. The minimum number of expected voyages falling under the scope of this regulation is 240 in accordance with ship's schedule.

As it concerns the fuel types used in ship's engines, it should be stated that both main and auxiliary engines consume all the fuel types presented in the Literature Review and no potential engine retrofit will be needed. Therefore, the company in order to cope with international and European regulations has implemented the "bunkering switch" process.

3.4 Artificial Neural Networks (ANN)

Artificial Neural Networks are non-linear empirical models and they are motivated by human's biological neural network features and functions as they are trying to simulate brain's learning ability, the flexible information processing and memory (IBM, 2018). These computational based models are considered Machine Learning models and find great application in various fields (i.e. aerospace, finance, transportation etc.) as they have the ability to learn from datasets and they are trained in order to forecast future events taking into account data from the past (Hagan et. all, 2016). ANN models are widely used as they solve complex problems and they produce better outcomes compared to other prediction methods by providing more accurate results in real-time systems (Graupe, 2007).

The network's architecture consists of neurons called nodes, which are the basic component of a neural network. These neurons mimic the biological neurons as they have the ability to learn the information acquired by the input, to process internally the information and finally to generate the output (Graupe, 2007). The neurons are organized into layers (inputs, hidden layers and outputs) and they are linked to each other through edges. These edges have weights, which are adjusted during training process (Barh, Khan and Davies, 2015). More precisely, there are input nodes (numeric data points), which consist the Input layer and they are considered as the input variables. In the Input neurons, no computation takes place as they receive data and transfer the information from the environment to the network (Barh, Khan and Davies, 2015). Furthermore, Hidden layers are formed also by neurons where the most information process of the network takes place and it is considered as linkage between the Input and Output layer (Amardeep, 2017).

It should be noted that the complexity of the model is clearly associated to the number of neuros in the hidden layers (Amardeep, 2017). The output of the hidden layer is dependent on the output of the Input layer multiplied with the weight associated to the corresponding edge (Amardeep, 2017). The weight refers to the strength of the connection between the input and the output and how the input determines the output (Barh, Khan and Davies, 2015). Moreover, the Output layer transmits the information learned by the network to the environment (Figure 7) (Barh, Khan and Davies, 2015).

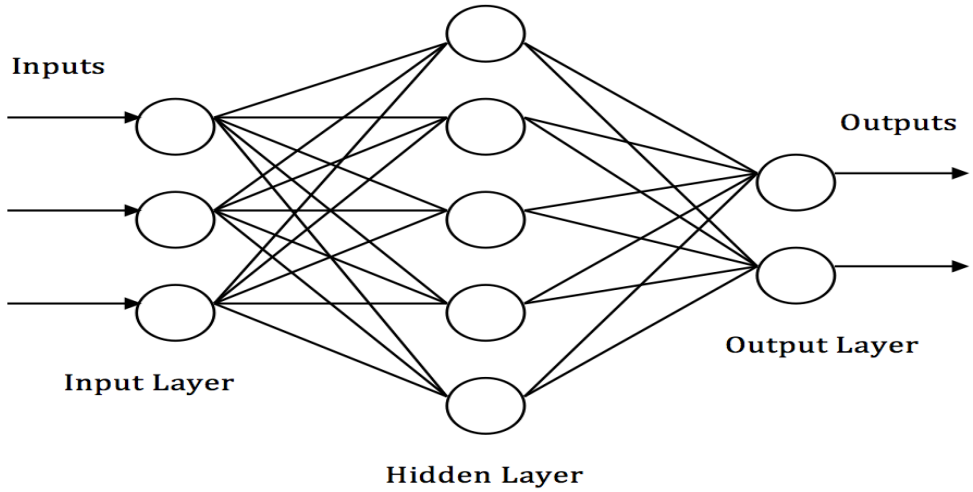

Figure 7: Mutli-layer Feed-forward Artificial Neural Network (source: author)

Another important element that plays crucial role to the neural network's performance during the training process is the activation or transfer function as it determines the output of the node and it is contained in the artificial neuron (Amardeep, 2017). The activation function not only determines the relationship between the nodes of input layer and the nodes of the hidden layer but also the interconnection between the nodes of hidden layer and the output (Amardeep, 2017). More specifically, the activation functions are either linear or non-linear mathematical equations converting the neuron's input into output signal (Amardeep, 2017). As it concerns the choice of ANN's activation function, there are many activation functions that can be applied in order to develop an ANN and the most commonly used are presented in Appendix C section (i.e. linear function, sigmoid or logistic activation function, hyperbolic tangent function, rectified linear unit etc.) However, the choice of the most suitable activation function depends on the complexity of the task that the network performs and the nature of the problem (Amardeep, 2017).

At this point, it is necessary to state that another feature of artificial neuron is the bias node, an extra input node, which takes a nonzero constant value and increases the flexibility of the model (Amardeep, 2017). The bias node determines the activation of the neuron as it is added to the summation of inputs multiplied by their weights and it is not affected by incoming connections from previous layers (Amardeep, 2017). Therefore, it is observed that a neuron is characterized by inputs, weights, bias and activation function and its structure is depicted in the Figure 8.

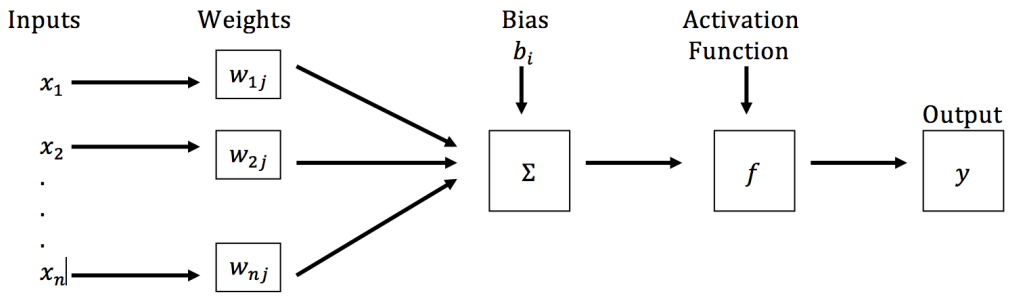

Figure 8: Structure of a neuron (source: author)

From all the above it is understood that the weights of inputs and the adding bias are summed up and the total weighted sum value of all inputs to the neuron is entered to activation function leading to the activation of the neuron (Barh, Khan and Davies, 2015). The total value of the neuron can be derived by the following equation:

$$\boldsymbol{u_i = \sum_{j=1}^{n} w_{ij} x_j + b_i} \quad \textbf{(3.1)}$$

where:
$w = weights\ of\ connection$
$x = inputs$
$b = bias$

Thus, the activation function takes the total weighted sum of inputs and the bias of the neuron (u_i) and performs all the necessary calculations in order to determine whether the neuron is activated or not (Barh, Khan and Davies, 2015). The output (y_i) of the activation function is provided by the following equation:

$$\boldsymbol{y_i = f(u_i)}, \quad \textbf{(3.2)}$$

or

$$\boldsymbol{y_i = f(\sum_{j=1}^{n} w_{ij} x_j + b_i)} \quad \textbf{(3.3)}$$

If the result from the activation function is above a certain limit then the neuron is considered activated (Barh, Khan and Davies, 2015). In case that the output from the activation function is below the predefined value, then the neuron is not fired (Barh, Khan and Davies, 2015).

Once the network's structure is developed, then the network is ready to be trained (Graupe, 2007). The most critical part of the training is the learning process of the network and two commonly used learning methods are observed, such as the supervised learning and the unsupervised learning (Graupe, 2007). More precisely, the supervised learning is considered the most utilized method, where a training pair (x, y) is set, meaning that for each input vector, an output is provided (Graupe, 2007). The predicted outputs are compared with the outputs already predefined and all weights (w_{ij}) are randomly set (Graupe, 2007). When the forecasted output is different from the desired one, then the network adjusts the weights until the target is achieved (Graupe, 2007). On the contrary, under the unsupervised learning the network is considered as self-organized where only input vectors are fed into the network (Graupe, 2007). Thus, the network is trained without any predefined data leading to the prediction of a target output (Graupe, 2007).

Another aspect that must be taken into account is the form of the ANN based on the flow of information and the number of hidden layers (Barh, Khan and Davies, 2015). As it concerns the flow of information the most commonly used structures are the Feed-Forward Networks, Radial basis function networks and Recurrent Neural Networks (Barh, Khan and Davies, 2015).

To begin, the Feed-Forward Network (FF) has one input layer, which is consisting of one, or more input nodes, then this layer is linked with the other hidden layer (multilayer feed-forward network) or directly to the output layer (single layer feed-forward network) (Barh, Khan and Davies, 2015). The Feed-Forward Network processes the information in one direction (forward) from the input layer to the output layer and no feedbacks (loops) are observed as each node in a layer is connected to every node of the previous layer (Barh, Khan and Davies, 2015). It is noteworthy to state, that the most commonly used learning method for Multilayered Feed-forward network is the Backward Propagation Algorithm (BPA), which is used to minimize the error (Amardeep, 2017). More specifically, during the training process when an error occurs at the output, then the recalculation proceeds backwards (from the last layer to the first) re-calculating the weights and the biases (Amardeep, 2017).

It is important to state that the error occurs when the network's output is different from the target set, as the network must provide a specific output (target) for each input (training pairs) (Amardeep, 2017). This can be justified by the fact that the weights are randomly

initialized (Barh, Khan and Davies, 2015). For this reason, BPA method is repeated until the adjusted weights result to minimum value of error, which is provided by the following formula (Amardeep, 2017):

$$\boldsymbol{E_i = \frac{1}{2}\sum_{i=1}^{n}(y_n - y_i)^2}, \quad \textbf{(3.4)}$$

where the y_n is the target output and $y_i$is predicted output.

There is a variation of learning algorithms that are applied in order to train the neural network, such as Gradient Descent, Resilient Backpropagation, Quasi-Newton, and Levenberg-Marquardt algorithms (Comert and Kocamaz 2017). The choice of the most proper algorithm is based on its learning rate in conjunction with its stability (Comert and Kocamaz 2017). The afore mentioned algorithms can be expressed by the following formulas:

- Gradient Descent: $\boldsymbol{x_{k+1} = x_k - a_k g_k}$, **(3.5)**

where: x_{k+1} is the new weight vector, x_k is the weights and biases, $a_k$is the learning rate and the $g_k$is the gradient of the error

- Resilient Backpropagation: $\boldsymbol{\Delta x_k = -sign\left(\frac{\Delta E_k}{\Delta x_k}\right)\Delta k}$, **(3.6)**

where: Δx_k is the change in weights vector, ΔE_k is the error function E at k and Δk is the change in bias.

- Quasi-Newton: $\boldsymbol{x_{k+1} = x_k - H_k^{-1} g_k}$, **(3.7)**

where: H_k is the Hessian matrix of the current weights and biases.

- Levenberg-Marquardt: $\boldsymbol{x_{k+1} = x_k - [J^T J + \mu I]^{-1} J^T e}$, **(3.8)**

where: J is the Jacobian matrix, e is the vector of errors (Comert and Kocamaz 2017)

Regarding the Radial basis function networks (RBF), they consist strictly of three layers, one input, one hidden and one output. The FF network's flow of information is applied also in the RBF network while the main difference is observed to the activation functions. More precisely, in the RBF network, the implemented activation function in the hidden layer is one of the radial basis functions, which introduces non-linearity (i.e. Gaussian, Multi-Quadric, Generalized, Multi-Quadric etc.) while the activation functions used in the output are the same with those employed in the MLP network.

Another commonly used ANN is the Recurrent Neural Network (RNN), which has a completely different flow of information from the FF and RBF (Comert and Kocamaz 2017).

The Recurrent Neural Network bears a closer resemblance to the biological neurons as the information processing has bidirectional flow (forward and backward) while their connections form a directed cycle (Graves, 2014). Moreover, the RNN has a memory capability as the previous iterations of inputs flow to network's internal state and influence each output (Graves, 2014).

Last but not least, the empirical evaluation of network's accuracy and performance is considered as an essential element for the successful implementation of the model. Several measures-metrics are used in order to examine the predictive ability of forecasting models. However the most commonly used methods are the Mean Squared Error (MSE), the Mean Average Percentage Error (MAPE) and the Coefficient of Determination (R^2) and are provided by the following equations:

$$\boldsymbol{MSE} = \frac{\mathbf{1}}{\boldsymbol{n}} \sum_{\boldsymbol{i=1}}^{\boldsymbol{n}} (\boldsymbol{A_i} - \boldsymbol{F_i})^{\mathbf{2}}\,, \tag{3.9}$$

$$\boldsymbol{MAPE} = \frac{\mathbf{100\%}}{\boldsymbol{n}} \sum_{\boldsymbol{t=1}}^{\boldsymbol{n}} \left| \frac{\boldsymbol{A_i - F_i}}{\boldsymbol{A_i}} \right|, \tag{3.10}$$

$$\boldsymbol{R^2} = \mathbf{1} - \frac{\sum_{\boldsymbol{i=1}}^{\boldsymbol{N}} (\boldsymbol{A_i - F_i})^{\mathbf{2}}}{\sum_{\boldsymbol{i=1}}^{\boldsymbol{N}} (\boldsymbol{A_i - \overline{F_i}})^{\mathbf{2}}}\,, \tag{3.11}$$

where: A_i is the actual value, the F_i is the predicted value and n is the number of data points.

3.5 Multiple Linear Regression Analysis (MR)

The most commonly used method for examining linear relationships between variables is the Multiple Linear Regression Analysis. Besides its statistical application, the MR is also employed as a predictive tool, hence a dataset is used in order a predictive mathematical model to be developed (Keith, 2015). This predictive technique will forecast the value of the dependent variable based on multiple explanatory variables (predictors) (Keith, 2015). To be more precise, the mathematical model used is linear and not only assesses the effect of two or more independent variables to one dependent variable but also predicts the value of the dependent variable taking into account the values of predictors and hence its equation is defined by the following formula:

$$\boldsymbol{y} = \boldsymbol{a} + \boldsymbol{b_1 x_1} + \boldsymbol{b_2 x_2} + \cdots + \boldsymbol{b_n x_n} + \boldsymbol{\varepsilon}, \tag{3.12}$$

where the y is the response or predicant variable, while the $x_1, x_2, \ldots x_n$ are the explanatory or independent variables. Moreover, $a, b_1, b_2 \ldots b_n$ are the regressions coefficients and ε is the

error (Keith, 2015). From the formula above, it is observed that the dependent variable has linear association with each one of the independent variables (Keith, 2015). Moreover, it is essential to state that in order to model the relationship between a predicant and a predictor by applying the MR, the following assumptions must be tested (Osborne and Waters, 2002):

1. The dependent and at least two predictor variables must be continuous.
2. Linearity between the dependent variable with each one of predictors. The predicant must be expressed as a linear function of independent variables.
3. The difference between the predicted and the actual values (residuals) must follow the Gaussian distribution.
4. Absence of multicollinearity, providing that regressors (independent variables) must not be tightly correlated to each other.
5. Absence of autocorrelation, providing that the residuals must be independent from each other. Therefore, the observations must be independent from their past values.
6. The residuals must be homoscedastic (constant variance of errors) (Osborne and Waters, 2002)

In case that one of the afore mentioned assumptions is not met, then the implications of the violation may lead to invalid or misleading results and thus the model must be adjusted (Keith, 2015). However, not all the violations have the same impact to the analysis. More specifically, a linearity violation is critical and it results to biased predictions, while a violation in the independence of residuals has impact only on standard errors (Keith, 2015). Additionally, a violation in homoscedasticity influences negatively the standard errors and the statistical significance of the model (Keith, 2015).

At this point it should be stated that the statistical procedure of the Least Square method is applied in order to reduce the squares of residuals occurred (Keith, 2015). Both the goodness of fit plays and the statistical significance play also a crucial role, as they reveal whether the regression model adequately describes the set of observations (Keith, 2015).

4. Data Analysis

In this section, the development and the selection of the most well-fitting ANN model in conjunction with its performance will be described and analyzed. Furthermore, the model's efficiency in accordance with the training and testing results will be provided. Additionally, the association between some operational parameters and the fuel consumption will be also investigated. On the top of that, a MR model will be employed and a performance comparison between these two models will be performed.

4.1 Operational, Design, Environmental Factors and Fuel Consumption

At this point, the integration between some operational, design and environmental parameters and the fuel consumption will be explored and analyzed in order to find which factors have impact on vessel's fuel consumption. More precisely, a correlation analysis will be conducted in order to examine the afore mentioned association. The potential relationship will be evaluated through the Pearson's correlation coefficient and a scatter plot, both will be performed under IBM SPSS Software. All the necessary data were derived from vessel's 322 voyage reports and the examined factors were selected based on Literature Review. The chart below (Figure 9) demonstrates the evolution of total fuel consumption in time.

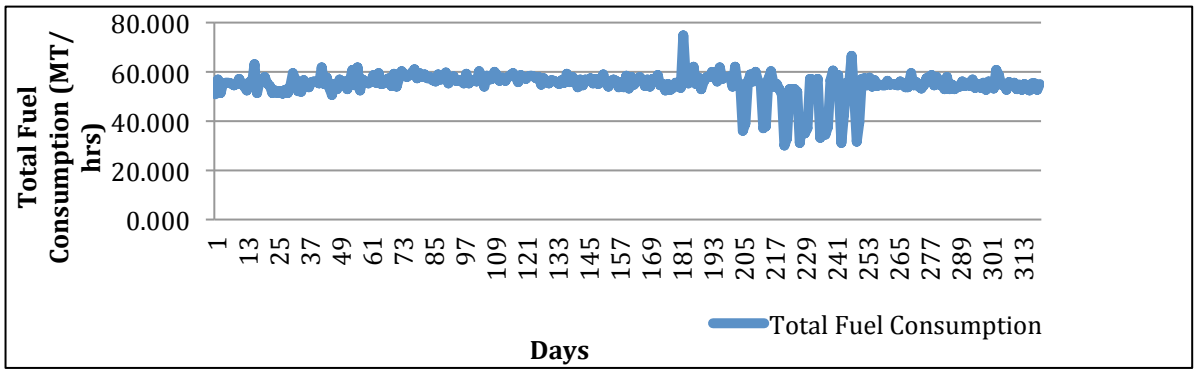

Figure 9: Evolution of Fuel Consumption (MT/hrs) in time (days) (source: author)

In accordance with the Literature Review, the total fuel consumption is affected by the parameters illustrated in the Figure 3 and in order to conduct our study, we chose some factors by each category in accordance with the data provided by the voyage reports.

To be more precise, from the ship design we chose Main Engines working hrs & LSFO consumption, from the operational performance, we selected the average speed of the vessel, the distance and the weight of the vessel (passengers, trucks, cars etc.) while from the environmental conditions we chose the Wind force expressed in B.N. In addition to the correlation between the aforementioned factors and the total fuel consumption, we carried out also a correlation analysis between total fuel consumption and the fuel consumption of Low Sulfur Oil (LSFO), Marine Gas Oil (MGO) and Heavy Sulfur Fuel Oil (HSFO) in order to perceive which of the previous fuels have greater impact on the total fuel consumption.

From the dataset of the voyage reports, some statistics of the total fuel consumption can be denoted. More precisely, in the examined case study the average fuel consumption is 54.93 MT/hr while its lowest value is 30 MT/hr and the highest fuel consumption is observed in the value 74.72 MT/hr.

The results from the correlation analysis between the total fuel consumption and the afore mentioned operational parameters are presented in the Table 4. First of all, it is observed that there is a strong uphill linear correlational relationship between the total fuel consumption variable and the LSFO fuel consumption of Main Engines as the Pearson correlation coefficient was found 0.919. This result shows that those two variables are tightly associated as the correlation coefficient value is very close to 1. This can be justified by the fact that during the most of the voyage the ship's main engines consume more LSFO as it is operating in European navigational waters where legislations obligate the operator to use fuel with low sulfur content.

Moreover, positive correlations are also observed between the total fuel consumption and both variables HSFO and MGO fuel consumptions with correlation coefficients r_2=0.373 and r_3=0.165 respectively. This outcome can be justified by the fact that the HSFO is consumed by main engines when the vessel is operating in international waters while the MGO is consumed during the vessel's stay at port for only 5hrs in conjunction with the fact that only auxiliary engines and boilers use this specific fuel.

Table 4: Correlation Analysis of Fuel Consumption

Correlations

		TTL_FUEL_CONS	ME_LSFO_FUEL_CONS	ME_HSFO_FUEL_CONS	MGO_FUEL_CONS	AVERAGE_SPEED	MILES	WIND	WEIGHTS
TTL_FUEL_CONS	Pearson Correlation	1	.919**	.373**	.165**	-.179**	.886**	.211**	.437**
	Sig. (2-tailed)		.000	.000	.003	.001	.000	.000	.000
	N	320	320	320	320	320	320	320	320
ME_LSFO_FUEL_CONS	Pearson Correlation	.919**	1	.079	-.089	-.012	.948**	.154**	.433**
	Sig. (2-tailed)	.000		.158	.112	.836	.000	.006	.000
	N	320	320	320	320	320	320	320	320
ME_HSFO_FUEL_CONS	Pearson Correlation	.373**	.079	1	.071	-.303**	.078	.297**	.055
	Sig. (2-tailed)	.000	.158		.208	.000	.163	.000	.329
	N	320	320	320	320	320	320	320	320
MGO_FUEL_CONS	Pearson Correlation	.165**	-.089	.071	1	-.256**	-.077	-.022	-.048
	Sig. (2-tailed)	.003	.112	.208		.000	.169	.691	.389
	N	320	320	320	320	320	320	320	320
AVERAGE_SPEED	Pearson Correlation	-.179**	-.012	-.303**	-.256**	1	-.014	-.447**	.204**
	Sig. (2-tailed)	.001	.836	.000	.000		.802	.000	.000
	N	320	320	320	320	320	320	320	320
MILES	Pearson Correlation	.886**	.948**	.078	-.077	-.014	1	.116*	.410**
	Sig. (2-tailed)	.000	.000	.163	.169	.802		.038	.000
	N	320	320	320	320	320	320	320	320
WIND	Pearson Correlation	.211**	.154**	.297**	-.022	-.447**	.116*	1	-.010
	Sig. (2-tailed)	.000	.006	.000	.691	.000	.038		.856
	N	320	320	320	320	320	320	320	320
WEIGHTS	Pearson Correlation	.437**	.433**	.055	-.048	.204**	.410**	-.010	1
	Sig. (2-tailed)	.000	.000	.329	.389	.000	.000	.856	
	N	320	320	320	320	320	320	320	320

**. Correlation is significant at the 0.01 level (2-tailed).

*. Correlation is significant at the 0.05 level (2-tailed).

(source: author)

The aforementioned observation can be explained by the fact that the MGO has the lower consumption as it is used while the vessel is at port and only by auxiliary engines, which are operating, for 5hrs providing only the power required for covering the hotel operations. From the other hand, the LSFO has the highest fuel consumption as it is consumed by vessel's main engines, which are operating for 8hrs in European waters, covering not only the hotel but also the propulsive demand. Although the HSFO is only consumed for 3,5hrs during the vessel's passage from international waters, it has stronger correlation with the total fuel consumption compared to MGO. This observation can be justified by the fact that the vessel has higher speed variations when she is sailing in high seas, resulting to higher engine's rpm fluctuations and consequently to higher fuel consumption, fact that is also confirmed by the findings of Gusti, and Semin (2016).

Additionally, the correlation coefficient between the examined variable and the distance (r_5=0.886) points out also a tight association. This can also be confirmed also by the

fact that the maximum value of the total fuel consumption (74.72 MT/hrs) is observed when the vessel reroutes for commercial reasons and calls the port of Corfu, covering a distance of 400 miles whilst the scheduled itinerary was 318 miles (Patra – Igoumenitsa – Bari). Therefore, under this case it is also provided that the fuel consumption is dependent on the distance covered, which is also depicted in the Figure 11.

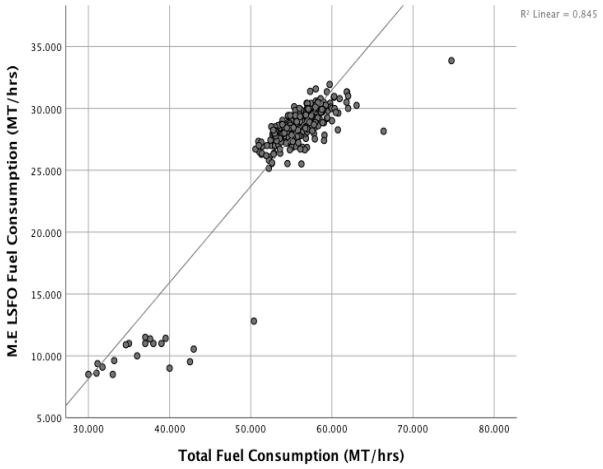

Figure 10: Scatterplot between Fuel Consumption and M&E LSFO Fuel Cons. (source: author)

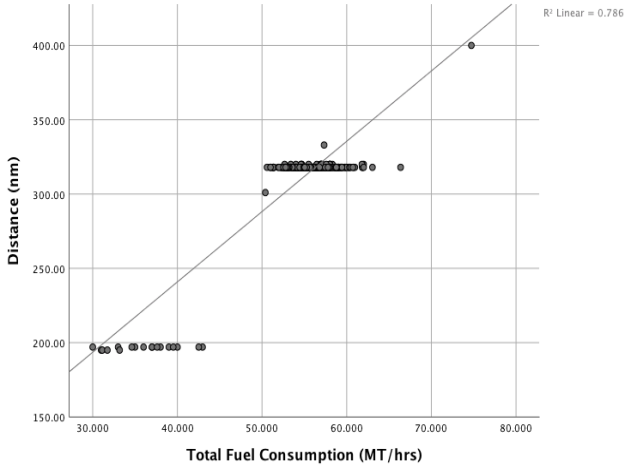

Figure 11: Scatterplot between Fuel Consumption and distance (source: author)

Further to the above, the values of r_6=0.211 and r_7=0.437, which are referred to the correlation coefficients between the fuel consumption and the variables of wind (BN) and weights respectively, also indicate a positive linear relationship between the examined variables. At this point it should be stated that the weight refers to the weight of cargo, the light ship and the weight of bunkers. The dataset from voyage reports provided the number of passengers, trailer, trucks, campers, moto, buses, cars and in order to assess the total weight of the cargo, we used IMO's conversion factors for Ro/Pax load calculation (IMO, 2019). The value of the r_7 coefficient depicts that the vessel's weight has impact on the fuel consumption, as the weight increases, the consumption rises as well.

As it concerns the Wind, the coefficient r_6 reveals that those variables are also associated and the fuel consumption is affected by the wind but it also demonstrates that those two variables do not perform at the same way, as the weather conditions do not have significant impact on fuel consumption. This can be proved by the fact that, on the one hand we didn't take into account the wind directions while on the other, the impact of the wave

effect cannot be estimated which is considered as the most important environmental factor according to the Literature Review.

Last but not least, there is a negative correlation between the examined variable and the speed r_4=-0.179. This observation implies that there is not a tight association between these two variables while they move in opposite directions. However, according to Literature Review, it is denoted that the speed and the fuel consumption has a non-linear relationship, fact that may justify the above observation.

The outcome of this statistical analysis indicates that the fuel consumption is tightly associated with the distance and the main engines' LSFO fuel consumption and consequently to engine's operating hours. Moreover, the weight and the weather conditions (wind) also affect the fuel consumption. However, the results provide that there is a negative association between fuel consumption and speed.

4.2 Design of the ANN model

In order this study to be conducted, an Artificial Neural Network (ANN) is developed and applied for the total fuel consumption prediction of the day ahead, which incorporates the consumption of LSFO, HSFO and MGO, which are used by the both the main and auxiliary engines, and boilers of the vessel. This ANN model is designed and developed by using Neural Net Fitting (nftool) provided by MATLAB Deep Learning Toolbox. The Figure below depicts the operation and the flow of information in the ANN.

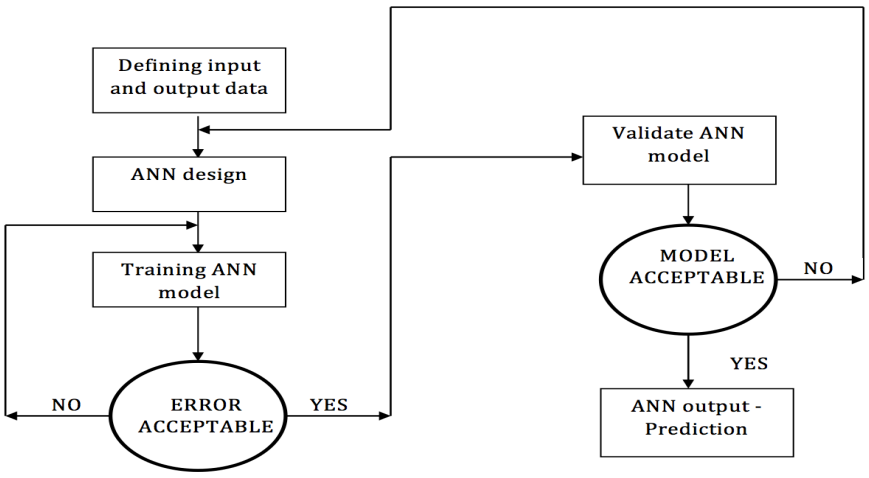

Figure 12: Operation of Artificial Neural Network (source: author)

The ANN model is developed based on the 322 observations provided by the voyage reports, which are referred to the period from 2nd January 2018 until 14th November 2018. A sample of 257 (80%) voyage reports for the period from 2nd January 2018 until 12th September 2018 were used as training data, where the neural network was learning, while the remaining 65 (20%) input data was selected in order to validate and test the model's performance and accuracy.

It is noteworthy to state here that the data used both for training and testing process are normalized before feeding the network. However, after the training and testing process, the output values will be also converted to normal values in order to be compared with the actual values of fuel consumption. More precisely, all the rescaled values of the data are ranging between 0.1 and 0.9 in accordance with the following min-max normalization equation:

$$\boldsymbol{X_n = \frac{X - X_{min}}{X_{max} - X_{min}}} \quad \textbf{(4.1)}$$

where, the X_n is the normalized data, X is the real value of the variable, while the X_{max} and X_{min} are the maximum and minimum real value of the data respectively.

After the rescaling of the data, the structure and the topology of the network must be identified. In our case, the Feed-forward structure of ANN with supervised learning algorithm is chosen to predict the total fuel consumption based on the fact that this structure guarantees the stability of the network and generalizes the input–output association by predicting values for inputs that it is not trained on. Hence, it is understood that the proposed ANN network has the topology of a Multilayered (more than one layers) Feed-Forward Neural network (ML FFNN).

The most important part for ANN modeling is to identify the optimum network architecture, as it t influences also its performance and it is related to the number of hidden layers, neurons in the hidden layers and the training algorithm. Such will be achieved through the identification of the number of input data (variables), the number of neurons in the hidden layers and the output data (prediction). The structure of the proposed ANN is determined by trying various combinations in order to carefully choose the most appropriate architecture for the examined problem.

As it concerns the input neurons, three different scenarios were taken into account in order to configure the ANN model. Under these three scenarios, different numbers of input neurons were taken into consideration and varied between 2 and 12 input variables while there is one output data. These three scenarios will be further elaborated in the next section. Moreover, the proposed neural network consists of one input, one hidden and output layer (three layered neural network) and the number of neurons in the hidden layer are varied between 2 and 30.

At this point it should be stated, that hyperbolic tangent sigmoid, the logarithmic sigmoid ($tansig(n) = \frac{2}{[1+\exp(-2^n)]-1}$), function is applied as activation function in the trained neural network both in hidden and output layer in order the network to learn the non-linear relationship between the input variables and the output. This activation function is similar to hyperbolic tangent (tanh(n)) and also related to bipolar sigmoid, and the range of its inputs and outputs is varied between -1 and +1. According to MathWorks (2018), under this specific activation function ('TANSIG') the learning process of the ANN is running faster compared to the hyperbolic tangent activation function. However, the results make small numerical differences apparent (MathWorks, 2018).

In addition, the Levenberg-Marquardt (LM) is used as the network's backpropagation learning algorithm, which is a combination of gradient descent and Gauss–Newton minimization methods. LM algorithm ('TRAINLM') is applied in order not only to update the weights and biases but also to reduce the sum of square errors functions with respect to new adjusted weights of the network. Hence, it is understood that the proposed neural network will be trained under the LM learning algorithm in order a specific input to meet the predefined output (target). The choice of the LM algorithm out of other learning methods is based on the fact that the LM is considered as the most suitable to solve non-linear problems in networks with few weights in conjunction with its fast convergence (MathWorks, 2018). The LM algorithm is provided by the formula (3.8) presented in the Methodology section.

Moreover, the training of network will be completed after 1000 epochs, fact that indicates that the learning algorithm will train the data for 1000 iterations until the error is minimized. The Table 5 summarizes the fundamental characteristics of the ANN configuration.

Table 5: ANN Configuration

Parameters	Specification
Nr. Of total layers	3
Input Layer Neurons	2 -12
Hidden Layer Neurons	2 - 30
Output Layer Neurons	1
Learning Algorithm	Levenberg-Marquardt (LM)
Activation Function	Hyperbolic tangent sigmoid (tansig(n))
Epochs	1.000
Performance Functions	Mean Absolute Percentage Error (MAPE)

(source: author)

From all the above, it is noted that the training process of the Feed-Forward backpropagation network can be summarized to the following 5 basic stages:

1. The weights of the neurons are set randomly.
2. The feed-forward process, where the information flows from the input, to the output through the hidden layer. At this stage the input vectors are entered into the network, they will be transformed in the hidden layer, and an output will be produced, while all the weights are fixed.
3. Backpropagation process is performed through the LM learning algorithm
4. Weights and biases are adjusted until the error value to be minimized and the network provides the best approximation of the predefined output.
5. Test for network's stopping condition is applied. In our case, the criterion for stopping network's training is determined by the number of epochs.

Another feature that must be taken into account is the performance of the network, fact that will be determined by using Mean Absolute Percentage Error (MAPE). The overall accuracy of the model will be measured by MAPE both during the training and testing process and will be expressed as a percentage as it is the most widely used error indicator. At this point it should be stated that the choice of MAPE was based on the fact that there were no extreme values in the dataset. The MAPE is given by the formula (3.10) provided in Methodology section. Hence, the selection of the most suitable ANN model depends on the

value of MAPE as the model with the lowest MAPE value during the testing period will be used for forecasting.

4.3 The Architecture of ANN model

As it has stated earlier, the choice of the most suitable architecture is a major challenge for the efficiency of the neural network. For this reason, three different scenarios were investigated and 90 different neural networks were developed and tested in order to conclude to the most suitable ANN model.

The choice of the most optimum ANN structure will be determined by running various combinations of architectures during the training and the testing process. More precisely, in the first scenario, 30 neural networks are developed, trained and tested by assuming that the fuel consumption prediction is based on previous fuel consumption values. In the second scenario also 30 networks were built and the fuel consumption is predicted based on previous and future values of exogenous input variables. The third and last scenario is considered as combination of two previous scenarios as the 30 networks included both previous fuel consumption values and previous and future values of exogenous input variables. However, the selection of the ANN network will be determined during the testing process through the employment of error method. It is noteworthy to state here that no fixed number of hidden nodes was selected and thus it will be also determined by the model's MAPE during the testing process. At this point it should be stated that the testing results show the ability of the model to generalize.

1st Scenario

In this scenario, we assume that the fuel consumption is related to previous fuel consumption values. In order to examine this specific scenario, the degree of association between the fuel consumption values at different points in time must be investigated. Therefore, an Autocorrelation Analysis (serial correlation) will be carried out between fuel consumption's current values and its preceding values and it is plotted from a lag of 30 days in order to determine whether the fuel consumption values are influenced by their historical values (Figure 13).

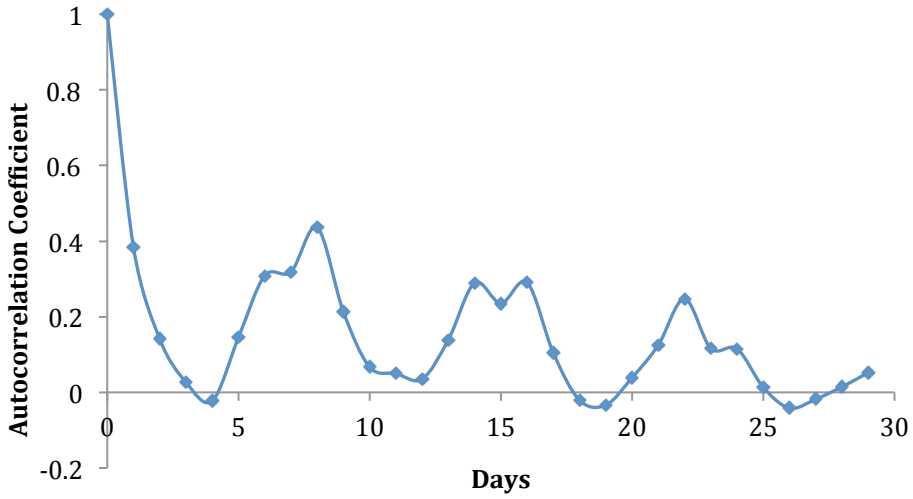

Figure 13: Autocorrelation coefficient for 30 days (source: author)

At this point, it is necessary to mention that variables are considered correlated when the Pearson correlation coefficient values are close to r_0=0.90, which reflects that variables have a strong correlational association. The findings of the Pearson coefficient are depicted in the diagram below. However, the results reveal the absence of autocorrelation between fuel consumption values for the afore-mentioned lags, fact that may lead to low prediction accuracy.

As it concerns the development of the ANN network, we choose as input neurons the total fuel consumption at the d-1 (day 1) with value 0.38 and d-8 (day 8) with value 0.43. At this point, it should be mentioned that aforementioned values were derived from autocorrelation coefficients for these two specific days and we assume that the neuron output of the neural network is the fuel consumption of the day (d). Therefore, it is understood that the developed neural network under this scenario has 2 neurons in the Input layer. As it concerns the number of neurons in the hidden layer, the network will be trained for different number of nodes. This process will be repeated for various numbers of nodes in the layer up to 30. Nevertheless, the optimal number of neurons in the hidden layer will be determined after applying the MAPE error method. The graph below (Figure 14) depicts the results derived from testing and training process, the x-axis shows the number of neurons in the hidden layer while the mean absolute percentage errors are represented in the y-axis.

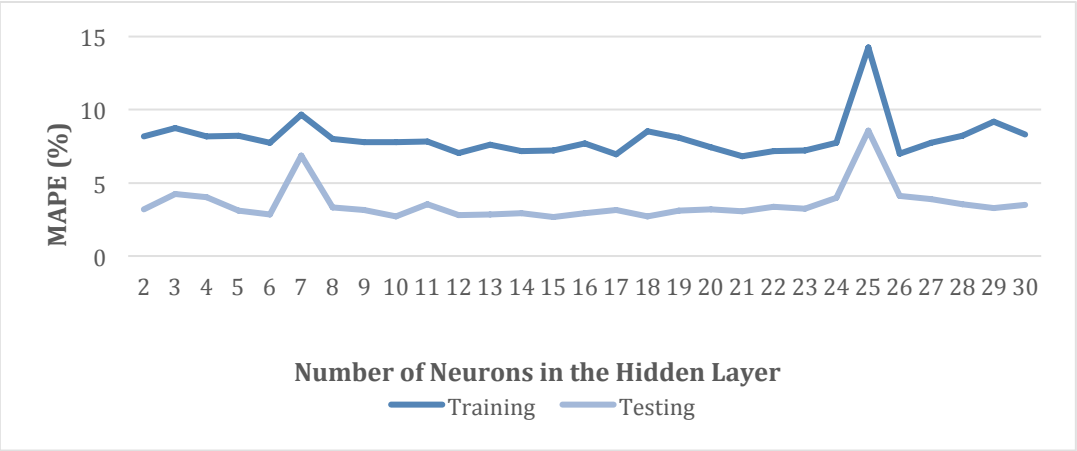

Figure 14: MAPEs for the 1st Scenario (source: author)

From the Figure 14 it is observed, that both the reduction and the increase in the number of nodes in the hidden layer do not improve the training performance of the neural network. Furthermore, high difference in MAPE values between the training and testing period are also illustrated in the graph. The number of neurons in the hidden layer will be determined by the lowest percentage of the error in the testing process. We may notice that the lowest percentage is 2.66% and it provided when the hidden layer has 15 neurons. Hence, the ideal architecture for this FFNN under these specific scenario compromises 2 input neurons, 1 hidden layer with 15 neurons and 1 output neuron (2-15-1NN). The network's stucture under MATLAB Neural Net Fitting ('NFTOOL') is presented in the Appendix D.

2nd Scenario

Under this scenario, we assume that the fuel consumption depends only on exogenous factors and not on its past values. So, the ANN network will be developed in accordance with the variables presented in the 4.1 section of the Methodology. More precisely, the examined variables are the average vessel's speed, wind force (BN), the number of passengers, Main Engine Hours and total Consumption of LSFO, the distance. It is necessary to point out that the number of passengers is taken into account as it has impact on the vessel's weight and consequently to the total fuel consumption in accordance with the previous studies presented in the Literature Review section. Moreover, under this scenario, the previous day values (timed step 1) of the aforementioned variables are also used for the development of the ANN. Hence, it is assumed that the input variables are the following:

- Input 1: Average Speed of the vessel at the day d-1
- Input 2: Average Speed of the vessel at the day d
- Input 3: Wind Force at the day d-1
- Input 4: Wind Force at the day d
- Input 5: Number of passengers at the day d-1
- Input 6: Number of passengers at the day d
- Input 7: Main Engine Hours & Total Consumption LSFO at the day d-1
- Input 8: Main Engine Hours & Total Consumption LSFO at the day d
- Input 9: Distance at the day d-1
- Input 10: Distance at the day d

As it concerns the nodes in the hidden layer, they were varied also between 2-30 neurons during the training and testing method. However, also in this scenario, the MAPE error method will allocate the number of neurons in the hidden layer. From the Figure 15 where the graph is illustrated, it is shown that the value of 2.16% is the lowest percentage of error during the testing period and it is observed when the hidden layer consists of 15 nodes.

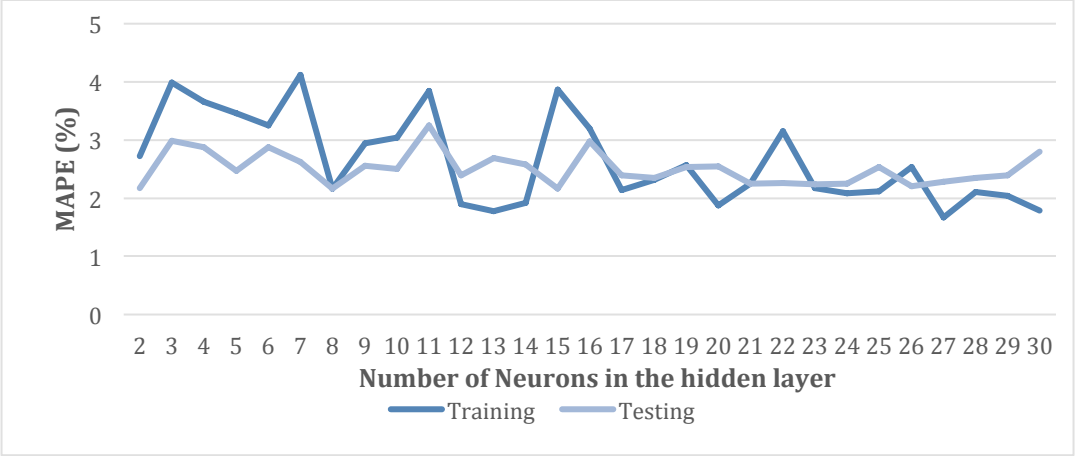

Figure 15: MAPEs for the 2nd Scenario (source: author)

Thus, it is concluded that under this scenario the ANN with the best predictive performance consisted of 1 input layer with 10 neurons, 1 hidden layer with 15 neurons and 1 output layer (10-15-1NN). The FFNN's structure under this scenario developed by MATLAB 'nftool' is provided in the Appendix D.

3rd scenario

As it is already stated, the third scenario is considered as a combination of the previous two scenarios. More precisely, we assume that the fuel consumption is related not only to exogenous factors and their previous day values (d-1) but also to its previous values. Hence, the ANN model will have 12 nodes in the input layer, 1 hidden layer and 1 output layer. Therefore, the ANN is tested based on the following input variables:

- Input 1: Average Speed of the vessel at the day d-1
- Input 2: Average Speed of the vessel at the day d
- Input 3: Wind Force at the day d-1
- Input 4: Wind Force at the day d
- Input 5: Number of passengers at the day d-1
- Input 6: Number of passengers at the day d
- Input 7: Main Engine Hours & Total Consumption LSFO at the day d-1
- Input 8: Main Engine Hours & Total Consumption LSFO at the day d
- Input 9: Distance at the day d-1
- Input 10: Distance at the day d
- Input 11: Total Fuel Consumption at the day d-1
- Input 12: Total Fuel Consumption at the day d-8

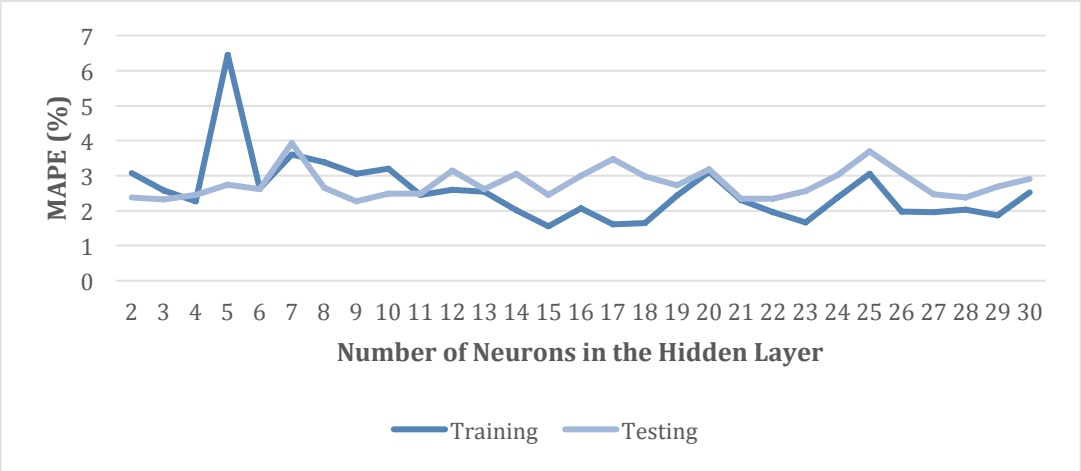

Figure 16: MAPEs for the 3rd Scenario (source: author)

As it concerns the neurons in the hidden layer, the Figure 16 depicts that during the testing process, the lowest percentage of MAPE has the value of 2.31% and it is observed when the neural network has 9 neurons in the hidden layer. Therefore, under this case the optimum ANN structure consists of 12 neurons in the input layer, 9 neurons in the hidden layer and 1 output neuron (12-9-1NN). The architecture of the FFNN under this case is also provided in the Appendix D.

4.4 Selection of ANN model

In the previous section, three different scenarios were conducted and 90 networks have been tested in order to choose the final optimal configuration of the ANN model. The proposed ANN model will be the one with lowest MAPE value during the testing period. The lowest mean absolute percentage error is occurred under the 2nd scenario with MAPE value 2.16%. Therefore, the network's architecture of the developed ANN model is 10-15-1NN for the prediction of the fuel consumption, which indicates the number of nodes in the input, hidden and output layer respectively.

Further to the above, it is important to state that the most well-fitted model provides also the most optimal values of weights fact that leads also to error reduction. Hence, it is understood that the model's predictive accuracy and performance it is related not only to its architecture but also to the optimum adjustment of weights and biases. Moreover, it is considered necessary to state here that the proposed model is not over-fitted as during both the training and testing process, provides good results, fact that outlines also its generalization ability. The final structure of the ANN model is presented in the Figure 17 while the Network's architecture under MATLAB Neural Net Fitting ('NFTOOL') is presented in the Appendix D section.

As already stated in the previous chapter, the activation function is the Hyperbolic tangent sigmoid both in the hidden and output layer as it evaluates better the association of nonlinear phenomena such as the relationship of the fuel consumption with various design, operational and environmental parameters, fact that is also confirmed by the literature.

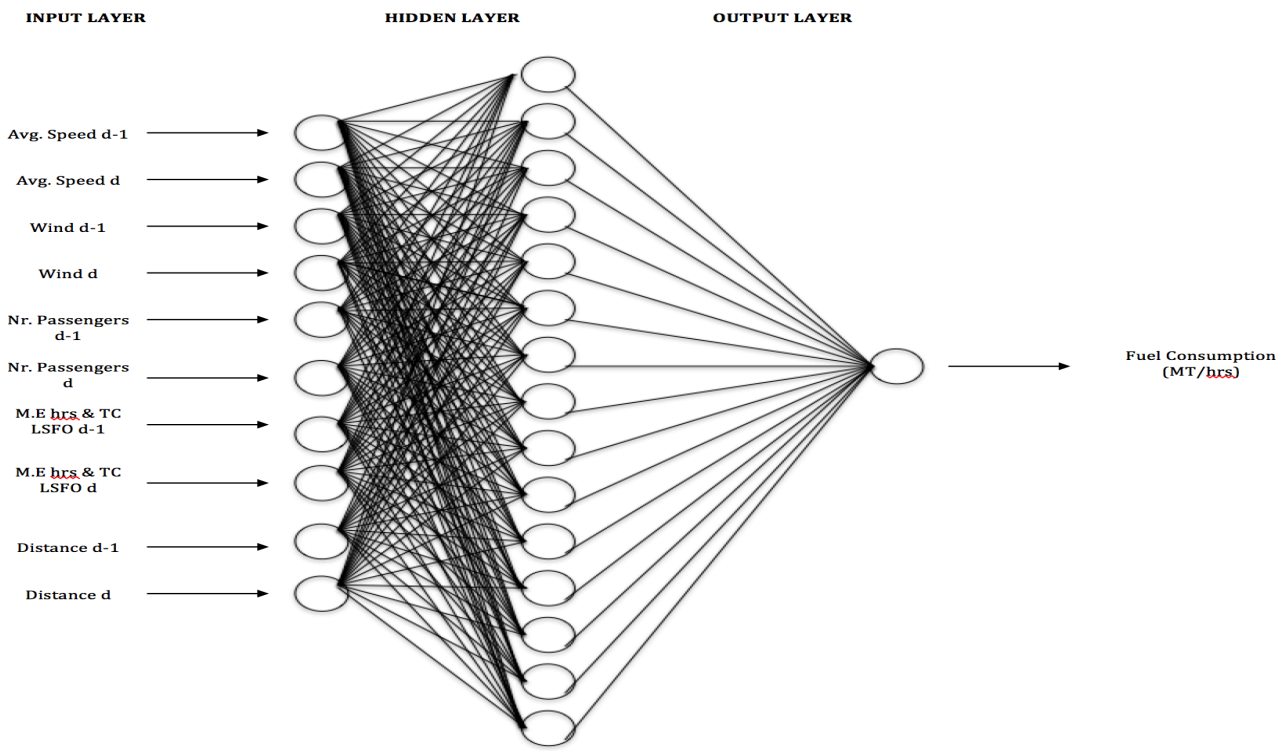

Figure 17: Schematic Diagram for the FFNN (source: author)

From all the above, it is observed that the 10-15-1NN model is the most accurate model in terms of the predictive accuracy, generalization ability and overall performance. The MAPE method was used for explaining and exploring the model's predictive performance and accuracy during both the training and testing process. As it concerns its generalization ability, the proposed model responded to the unknown data subset during the testing in the same way it did during the training process, providing also good results.

The graph below (Figure 18) depicts the mean absolute percentage errors for the three scenarios. More specifically, in the first scenario the MAPE is estimated 2.66%, while in the second and the third scenario the MAPE is 2.16% and 2.31% respectively. Hence, the lower the MAPE, more robust the predictive model is. Moreover, the overall performance of the model can also be outlined by the fact that lower variations in the values of MAPE are observed under the second scenario.

Moreover, it is noteworthy to state that the occurrence of 2.16% of error may be justifiable due to the fact that the total vessel's resistance was not taken into account as input variable as this component has impact both on fuel consumption and the speed of vessel.

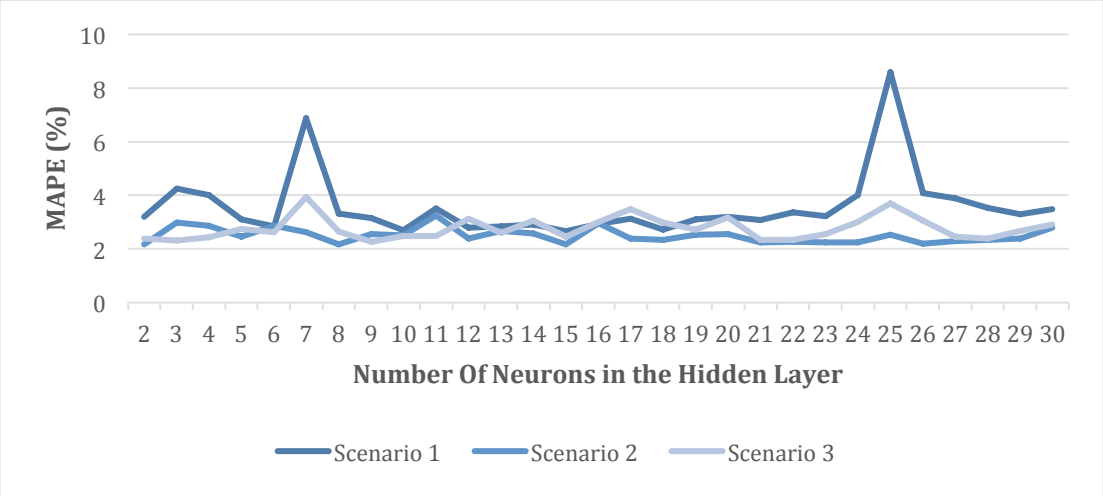

Figure 18: Comparison of MAPEs (source: author)

In addition to all above, a comparison between the predicted and actual values of fuel consumption is also conducted. The results derived from the comparison are illustrated in the graph below (Figure 19), where it is observed that predicted values of the proposed ANN are very close to the actual values and both follow the same trend during the testing process (65 observations). However, it is noteworthy to state that the proposed FFNN model has better generalization capability and accuracy when the model predicts the fuel consumption for the day ahead rather than when the ANN runs for long term fuel consumption prediction.

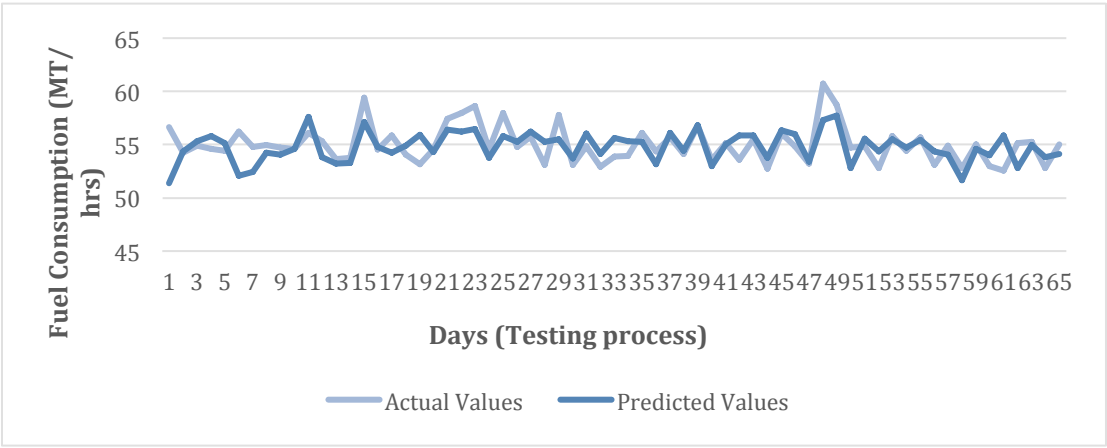

Figure 19: ANN predicted values vs actual values (source: author)

The findings from the employment of the ANN model revealed that the fuel consumption is more related to exogenous factors rather than to its preceding values. Additionally, the predictive model is an autoregressive model as its learning process depended on timed steps by using as input variables also the previous day values of the variables used. Thus, the 10-15-1NN model provides better prediction results for the fuel consumption for the day ahead when several parameters are known, consequently this tool can also be used for the estimation of the ship-generated emissions. Therefore, the total fuel consumption can be expressed as a function of operational, design and environmental parameters (average vessel speed, wind force, number of passengers, distance, and M.E Hours & Total Consumption of LSFO). More precisely, the hyperbolic tangent sigmoid is given by the following equation:

$$\boldsymbol{tansig}(\boldsymbol{U_i}) = \frac{\mathbf{2}}{[\mathbf{1}+\mathbf{exp}(-\mathbf{2}^{U_i})]-\mathbf{1}}, \quad \textbf{(4.2)}$$

where Ui is given by the following function:

$$\mathbf{U_i} = \textbf{average vessel speed d} - \mathbf{1} \times \mathbf{C_{1i}} + \textbf{average vessel speed d} \times \mathbf{C_{2i}} + \textbf{wind force d} - \mathbf{1} \times \mathbf{C_{3i}} + \textbf{wind force d} \times \mathbf{C_{4i}} + \textbf{number of passengers d} - \mathbf{1} \times \mathbf{C_{5i}} + \textbf{number of passengers d} \times \mathbf{C_{6i}} + \mathbf{M.E\ hrs}\ \&\ \mathbf{TC\ LSFO\ d} - \mathbf{1} \times \mathbf{C_{7i}} + \mathbf{M.E\ hrs}\ \&\ \mathbf{TC\ LSFO\ d} \times \mathbf{C_{8i}} + \textbf{distance d} \times \mathbf{C_{9i}} + \textbf{distance d} - \mathbf{1} \times \mathbf{C_{10i}} \quad \textbf{(4.3)}$$

Moreover, it should be stated that C_{ij} is referred to adjusted weights of the input layer while the function used in the hidden layer (15 nodes) is given by the following equation:

$$\boldsymbol{K_i} = \sum_{l=1}^{n=15} \boldsymbol{tansig}\ (\boldsymbol{U_i}) \times \boldsymbol{lw_i}, \quad \textbf{(4.4)}$$

The above stated equation provides the outputs from the hidden layer, which is consisted by 15 neurons, and 1 bias (b_2) while the normalized value of the output is represented by the following Equation (20).

$$\boldsymbol{y_i} = \boldsymbol{f}(\boldsymbol{U_i}) = \frac{\mathbf{2}}{[\mathbf{1}+\boldsymbol{exp}(-\mathbf{2}^{K_i})]-\mathbf{1}}, \quad \textbf{(4.5)}$$

At this point, it should be stated that the predicted output values will be converted back into their original scale values using the equation (4.1).

4.5 Multiple Regression Model

In this section, a Multiple Linear Regression Analysis will be interpreted in order a mathematical model to be developed which will predict the fuel consumption. Moreover, the association between the predictors will be explored and examined.

The linear mathematical model will be used in order to understand whether the fuel consumption can be forecasted based on two or more independent variables. As already provided in the section 3.5 Multiple Linear Regression Analysis (MR), the linear regression equation is defined by the following formula:

$$y = a + b_1 x_1 + b_2 x_2 + \cdots + b_n x_n + \varepsilon$$

where the dependent y variable represents the total fuel consumption prediction while the independent variables $x_1, x_2, \ldots x_n$ are Main Engine hrs & LSFO Consumption, Average Speed, Wind and Pax. Hence, it is understood that the Multiple regression model (MR) will be developed and assessed with the same data sets used for examining the accuracy of the ANN.

At this point it is considered necessary to state that for the development of the MR model, the past values of the aforementioned variables weren't taken into consideration. Furthermore, it is important to state here that in order our Regression Model to be valid, the assumptions provided under the Methodology section are considered fulfilled and not violated.

In this study, the multiple linear regression analysis will be performed under IBM SPSS software by applying both enter and stepwise method for the selection process. Although, it is noteworthy to mention here that in order to run the MR analysis the original variables are converted into standardized values (z-scores) and it is provided by the following formula:

$$\boldsymbol{z = \frac{x-\mu}{\sigma}}, \qquad \textbf{(4.6)}$$

where x is the variable's variable, μ is the population mean value and σ is the standard deviation.

The overall MR model accuracy and the how well the regression line fits will be determined by the coefficient of determination (R^2) and its values must range between 0 and 1, where values closer to 1 indicates a perfect fit. Another aspect that must be evaluated is the

significance of the model which will be determined by the p-values by taking into consideration that the level of significance is a=0.05.

Moreover, it should be stated that from the Table 4 *"Correlation analysis of fuel Consumption"* where correlation coefficients were presented, it is observed that the predictor variables "Main Engine & Total LSFO Consumption" and "Miles" are perfectly correlated with r=0.998, a fact which indicates the occurrence of multicollinearity in the regression model. Hence, the independent variable "Miles" is omitted from the MR analysis.

In addition to all above, a stepwise regression procedure will be also applied in order to identify which predictor variables add variability to the model resulting in the increase of R squared. As a result, the Multiple Regression Analysis will be divided into two categories concerning the selection process (enter and stepwise) by which the predictor variables are entered in the equation.

Under the enter method selection process, all predictor variables are entered in the equation simultaneously and the results from the Multiple Linear Regression Analysis performed under SPSS are depicted in the table below (Table 6).

Table 6: Model Summary (enter method)

Model Summary (enter method)					
Model	**R**	**R Square**	**Adjusted R Square**	**Std. Error of the Estimate**	**Durbin-Watson**
1	.911[a]	.831	.819	1.16219	2.118

(source: author)

It is observed that the R^2 is 0.831, fact that shows that the relationship between the dependent and the predictor variables is strong enough, as that the 83% of the variation of the Total Fuel Consumption is linearly explained by the predefined independent variables. The remaining 17% of the variation in Total Fuel Consumption can be explained by other factors such as the vessel's total resistance, hull roughness etc. Another factor that must be taken into account is the Adjusted R square which is not much lower than the R Square, fact that shows that the regression model can be generalized to the population. Hence, the 81% of total variance of the response variable can be explained by the model.

Moreover, from Durbin-Watson value d=2.118, it is assumed that there is no linear autocorrelation in residuals, as it falls within the range of 1.5 and 2.5. Moreover, the Standard error represents the regression error. In our case, S_e=1.16 provides that the 1.16% of variance in the Total fuel consumption cannot be explained by the regression model. Therefore, it is understood that the S_e is not high enough leading to the fact that the values are well-fitted to the regression line.

From the ANOVA Table (Table 7) we may examine the p-value in order to evaluate the significance of the regression model and whether the predictor values contribute significantly to the prediction of the total fuel consumption values. It is observed that the model's p-value accounts for 0.000 while the level of significance is a=0.05, hence the p-value is much lower than the level of significance. As a result, it is proved that the developed model is significant.

Table 7: ANOVA Table (enter method)

ANOVA (enter method)						
Model		**Sum of Squares**	**df**	**Mean Square**	**F**	**Sig.**
1	**Regression**	397.160	4	99.290	73.510	.000[b]
	Residual	81.042	60	1.351		
	Total	478.202	64			

(source: author)

From the table below (Table 8), the contribution of the independent variables to the model is indicated by the Column "*Sig"*. More precisely from predictors' p-values, it is observed that almost all independent variables significantly contribute to the regression model. However, only the Wind variable with p-value 0.424 does not contribute. Moreover, from the Column Variation Inflation Factor (VIF), the absence of multicollinearity is denoted, as only when the VIF ranges between 5 and 10 denotes the occurrence of multicollinearity in the model.

Furthermore, the B column is used in order to develop our regression model, as the values in the column are replacing the coefficients. These coefficients represent the association between the total fuel consumption and the independent variables. However, from the Table 8, it is denoted that the predictor "Average Speed" has negative coefficient, fact that

indicates the negative association between this variable and the predicant. This observation can be justified by the fact that the speed reduction can lead to higher fuel consumption due to the increase in the hull resistance and consequently to an increment in Effective Horsepower (Górski, Abramowicz-Gerigk and Burciu, 2013).

Table 8: Regression Analysis Outcomes (enter method)

Coefficients (enter method)								
Model		Unstandardized Coefficients		Standardized Coefficients	t	Sig.	Collinearity Statistics	
		B	Std. Error	Beta			Tolerance	VIF
1	(Constant)	55.217	.144		383.043	.000		
	Zscore(ME_LSFO_fc)	1.871	.179	.684	10.466	.000	.661	1.514
	Zscore(avg_speed)	-.884	.195	-.323	-4.538	.000	.556	1.799
	Zscore(wind)	.179	.223	.066	.805	.424	.425	2.351
	Zscore(pax)	.475	.149	.174	3.178	.002	.944	1.059

(source: author)

Therefore, from all the above stated, the our regression model will the following form:

$$\boldsymbol{Fuel\ consumption = 55.217 + 1.871 * ME\ LSFO\ fuel\ consumption + 0.179 * Wind - 0.884 * Speed + 0.475 * Pax} \quad \textbf{(4.7)}$$

At this point, stepwise selection process will be performed in order to identify all the explanatory variables that significantly influence the dependent variable. From the Table 9, where the model summary is illustrated, the results from the regression analysis indicate that the model with the highest R squared value (0.829) is the third one which incorporates the variables: average speed, M.E & LSFO Fuel Consumption and passengers, while the variable Wind is omitted from the regression analysis as it does not significantly contribute to the model's ability to predict the fuel consumption. This observation was also confirmed when applying enter method.

Table 9: Model Summary (stepwise method)

Model Summary (stepwise method)					
Model	**R**	**R Square**	**Adjusted R Square**	**Std. Error of the Estimate**	**Durbin-Watson**
1	.838[a]	.701	.697	1.50545	
2	.895[b]	.800	.794	1.24079	
3	.910[c]	.829	.820	1.15883	2.065

(source: author)

The coefficients and the variables used in the three regression models are illustrated in the Table 11 provided in the Appendix E. Furthermore, it is also denoted that only the variables with p-value more than 0.05 were entered in the model. More precisely, from the t values it is observed that the strongest predictor is the Main Engine hrs & LSFO total consumption, which is also confirmed by the Literature Review as fuel consumption is tightly associated with the main engine's working hours in conjunction with the LSFO fuel usage. It is denoted also that in the stepwise process, the "Average Speed" has a negative association with the dependent variable. The results also revealed the absence of multicollinearity in the regression model. Furthermore, the Figure 20 shows the interpretation of the Scatter Plot where the relationship between the actual and predicted values of the fuel consumption during the training and the testing process is depicted (322 observations). It should be stated that the x-axis shows the Fuel Consumption actual values while the y-axis represents the predicted values of the fuel consumption. A positive slope is clearly observed, fact that reflects the uphill positive relationship. Nevertheless, it should be stated that some outliers can be identified.

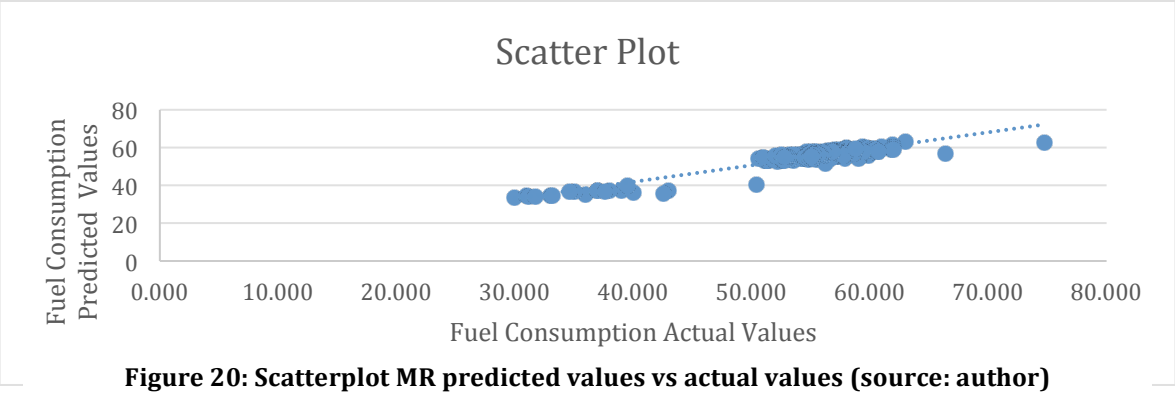

Figure 20: Scatterplot MR predicted values vs actual values (source: author)

At this point, it is considered necessary, a comparison between the Feed-forward Neural Network model and the Multiple Regression model to be performed. More precisely, the graph below (Figure 21) shows the predicted and the actual values of Fuel Consumption for both the FFNN and MR models during the testing process (65 observations).

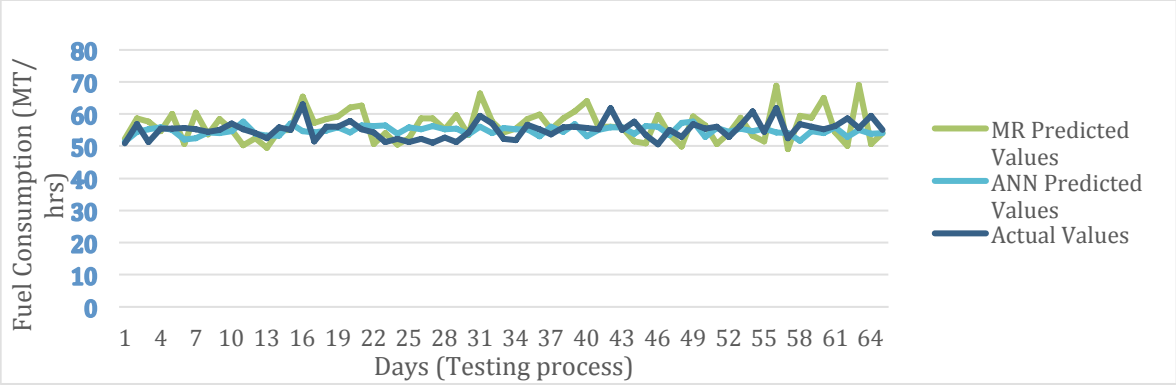

Figure 21: ANN & MR predicted values vs actual values (source: author)

It is observed that the predicted values of both models are very close to the actual values, however under FFNN model the values follow the same trend during the testing process fact that reflects that the FFNN model has higher prediction accuracy compared to MR model. The aforementioned can also be confirmed by the fact that the MAPE from the MR model is 2.54% while the MAPE for the ANN is 2.16%.

Table 10: MAPE for ANN and MR models (training & testing)

MAPE for ANN and MR models

	ANN		MR	
	Training	**Testing**	**Training**	**Testing**
MAPE	3.86%	2.16%	4.01%	2.54%

(source: author)

From the above analysis, it is concluded that both models are sufficient to predict the fuel consumption under different operating conditions (wind, speed, main engine working hours & LSFO fuel consumption), but the FFNN model has higher prediction accuracy compared to MR model due to the fact that the fuel consumption has non-linear relationship with the majority of these variables, which is also confirmed by the Literature used in this thesis.

5. Conclusion

One of the primary targets of the shipping sector is to minimize the fuel consumption, not only to mitigate the effect of increased fuel prices and but also to reduce ship generated greenhouse gases emissions. Generally, a vessel's energy efficiency strongly depends on the quantity of bunkers' consumption and as a result when the fuel consumption can be properly predicted, a fuel reduction along with an improvement in the energy efficiency of the vessel's operations can be achieved. The prediction of fuel consumption can significantly assist on indicating the over-consumption in terms of operating circumstances and can propose improved and qualitative operation strategies. Thus, the greenhouse gas emissions and costs of bunker fuel oils can be possibly decreased while the fuel can be also conserved for longer time.

This thesis is mainly focused on introducing and implementing both a computational and a statistical approach for fuel consumption prediction of a typical passenger vessel (Ro/Pax type), through the development of an ANN aiming to provide a tool for ship operators in choosing the most efficient measures towards achieving both ship's efficiency and sustained energy savings. The ANN model is very robust in examining the relationship between the fuel consumption and several input variables, as the forecasting error is very low, while when comparing its results with those arising from the use of an MR model, the ANN provided more accurate prediction results concerning the vessel fuel consumption.

The method, which is proposed, can be integrated into the energy management system of companies operating this type of vessels, and it can be used as a supporting tool that can assist ship operators on predicting the fuel consumption based on each specific operational condition. Hence, its implementation can be considered a fuel saving practice as the vessel's energy efficiency can be improved leading also to lower operational costs for the shipping company. Moreover, this model could be useful in terms of predicting the ship generated emissions.

This research has concluded to two main results. Firstly, it has shown that it is possible to predict the bunker fuel consumption of a ship by employing an ANN model. Secondly, it is observed that the fuel consumption is mainly related to exogenous parameters rather than to its own historical fuel consumption values. This is confirmed by the fact that the most optimal

neural network has as input variables several exogenous parameters important for the vessel's operation.

The proposed ANN is a multilayered feed-forward network (ML FFNN) with a LM backpropagation algorithm, and its structure is 10-15-1NN, which indicates the neurons in the input, hidden and output layer. Such was a result of investigating several ANNs with different architecture and of comparing their performances during the testing procedure, by taking into account their MAPE indicators. The result with the lowest MAPE error (2.16%) was obtained from the afore-mentioned one. Furthermore, a multiple linear regression (MR) model has been developed in order to lead to a fuel consumption prediction too. The MR model has also led to accurate results but when the performance of the MR and FFNN have been compared, it clearly showed that the most accurate prediction could be done through the FFNN as the MAPE error of the MR was 2.54%.

It is observed that an ANN model can be more accurate when forecasting the bunker fuel consumption compared to the linear model, as the fuel consumption has a non-linear relationship with the majority of the examined input variables. This has been also proved by previous studies and can now be re-confirmed. It is a general rule that the ANN model is used to mainly examine variables, which have a non-linear relationship, a fact that makes it workable for the case examined. At this point, it is necessary to state that the present research seems to result to more accurate prediction model, compared to the existing models presented in the Literature Review section. This can be justified by the fact that it presents an autoregressive model as its examinations also contain variables' values of the previous day (timed step), contrary to previous related researches, the values of which are only limited to these of the current day.

As a further proposal, a different ANN model, and more precisely the ANFIS model, could be introduced. This is proposed as the ANFIS model can provide better results by combining both the neural networks and fuzzy logic, requiring less training data and demonstrates faster convergence speed, compared with this of the ANN. Furthermore, the fuel consumption based on a FFNN model shall be examined in combination with CFD software. To be more precise, this should be done by taking into account several other variables such as the ship's total resistance in conjunction with the engine's rpm in order to develop a more robust data-driven predictive model.

6. References

Acomi, N. and Acomi, O. (2014). The Influence of Different Types of Marine Fuel over the Energy Efficiency Operational Index. *Energy Procedia*, [online] 59, pp.243-248. Available at: https://ac.els-cdn.com/S1876610214017408/1-s2.0-S1876610214017408-main.pdf?_tid=ec229f79-540a-4162-9f98-41977cbfa684&acdnat=1540485403_069dbb8ec6a92b3bc8591bdc1caba631 [Accessed 17 Oct. 2018].

Acomi, N. and Acomi, O. (2014). Improving the Voyage Energy Efficiency by Using EEOI. *Procedia - Social and Behavioral Sciences*, [online] 138, pp.531-536. Available at: https://www.sciencedirect.com/science/article/pii/S1877042814041548 [Accessed 11 Nov. 2018].

Aksoyoglu, S., Prévôt, A. and Baltensperger, U. (2015). Contribution of ship emissions to the concentration and deposition of air pollutants in Europe. *Atmospheric Chemistry and Physics Discussions*, [online] 15(21), pp.30959-30986. Available at: https://www.atmos-chem-phys.net/16/1895/2016/ [Accessed 20 Oct. 2018].

Amardeep, R. (2017). Training Feed forward Neural Network With Backpropogation Algorithm. *International Journal Of Engineering And Computer Science*, [online] 6(1), p.19861. Available at: https://www.ijecs.in/index.php/ijecs/article/.../1760/ [Accessed 16 Feb. 2019].

Aulinger, A., Matthias, V., Zeretzke, M., Bieser, J., Quante, M. and Backes, A. (2016). The impact of shipping emissions on air pollution in the greater North Sea region – Part 1: Current emissions and concentrations. *Atmospheric Chemistry and Physics*, [online] 16(2), pp.739-758. Available at: https://www.atmos-chem-phys.net/16/739/2016/acp-16-739-2016.pdf [Accessed 31 Oct. 2018].

Barh, D., Khan, M. and Davies, E. (2015). *PlantOmics: The Omics of Plant Science*. 1st ed. New Delhi: Springer.

Bal Beşikçi, E., Arslan, O., Turan, O. and Ölçer, A. (2016). An artificial neural network based decision support system for energy efficient ship operations. *Computers & Operations Research*, [online] 66, pp.393-401. Available at: https://www.sciencedirect.com/science/article/pii/S0305054815000842 [Accessed 17 Nov. 2018].

Banawan, A., Mosleh, M. and Seediek, I. (2013). Prediction of the fuel saving and emissions reduction by decreasing speed of a catamaran. *Journal of marine engineering and technology*, [online] 12(3), pp.40-48. Available at: https://www.researchgate.net/publication/263375305 Prediction of the fuel_saving_and_emissions_reduction_by_decreasing_speed_of_a_catamaran [Accessed 21 Feb. 2019].

Barrass, C. (2004). *Ship design and performance for masters and mates*. Oxford: Elsevier Butterworth-Heinemann, p.74.

Bialystocki, N. and Konovessis, D. (2016). On the estimation of ship's fuel consumption and speed curve: A statistical approach. *Journal of Ocean Engineering and Science*, [online] 1(2), pp.157-166. Available at: https://www.sciencedirect.com/science/article/pii/S2468013315300127 [Accessed 31 Oct. 2018].

Buschmann, R. and Nolde, L. (2018). *The World's Oceans*. Santa Barbara: ABC-CLIO, LLC, p.11.

Bomin. (2018). *Heavy Fuel Oil (HFO) | Glossary | Bomin*. [online] Available at: https://www.bomin.com/en/news-info/glossary/details/term/heavy-fuel-oil-hfo.html [Accessed 19 Oct. 2018].

Borkowski, T., Kasyk, L. and Kowalak, P. (2011). Assessment of ship's engine effective power fuel consumption and emission using the vessel speed. *Journal of KONES Powertrain and Transport*, [online] 18(2), p.32. Available at: https://pdfs.semanticscholar.org/cf18/c1d5a4fda71b9f49ab59d48f21ae6396d486.pdf [Accessed 14 Jan. 2019].

Carlton, J. (2012). *Marine Propellers and Propulsion*. 3rd ed. Burlington, MA: Butterworth-Heinemann, p.480.

Castelo Branco, R. (2011). *Basics of ship resistance*. Available at: https://www.slideshare.net/adsokant/basics-ofshipresistance [Accessed 11 Nov. 2018].

Castells Sanabra, M., Usabiaga Santamaría, J. and Martínez De Osés, F. (2013). Manoeuvring and hotelling external costs: enough for alternative energy sources?. *Maritime Policy & Management*, [online] 41(1), pp.42-60. Available at: https://www.tandfonline.com/doi/abs/10.1080/03088839.2013.782441 [Accessed 11 Nov. 2018].

Cesapo. (2016). *The Contribution of Pollutant Emission Sources on the Air Quality in Patras*. [online] Available at: http://www.cesapo.upatras.gr/Deliverables/Deliverable%205.2.1_final_report.pdf [Accessed 22 Oct. 2018].

Cofala, J., Amann, M., Heyes, C., Wagner, F., Klimont, Z., Posch, M., Schöpp, W., Tarasson, L., Jonson, J., Whall, C. and Stavrakaki, A. (2007). *Analysis of Policy Measures to Reduce Ship Emissions in the Context of the Revision of the National Emissions Ceilings Directive*. [online] European Comission. Available at: http://ec.europa.eu/environment/air/pdf/06107_final.pdf [Accessed 25 Jan. 2019].

Comert, Z. and Kocamaz, A. (2017). A Study of Artificial Neural Network Training Algorithms for Classification of Cardiotocography Signals. *Bitlis Eren University Journal of Science and Technology*, [online] 7(2), pp.93-103. Available at: http://ananth.in/docs/lmtut.pdf [Accessed 15 Feb. 1999].

Coraddu, A., Oneto, L., Baldi, F. and Anguita, D. (2017). Vessels fuel consumption forecast and trim optimisation: A data analytics perspective. *Ocean Engineering*, 130, pp.351-370.

Coraddu, A., Figari, M., Ghio, A., Oneto, L. and Savio, S. (2014). A Sustainability Analytics Matlab® Tool to Predict Ship Energy Consumption. *Conference: 13th Conference on Computer Applications and Information Technology in the Maritime Industries*. [online] Available at: https://www.researchgate.net/publication/267924673_A_Sustainability_Analytics_MatlabR_Tool_to_Predict_Ship_Energy_Consumption [Accessed 22 Feb. 2019].

Cullinane, K. (2011). *International handbook of maritime economics*. Cheltenham, U.K.: Edward Elgar, p.235.

Demirel, Y., Turan, O. and Incecik, A. (2017). Predicting the effect of biofouling on ship resistance using CFD. *Applied Ocean Research*, [online] 62, pp.100-118. Available at: https://www.sciencedirect.com/science/article/pii/S0141118716305685 [Accessed 10 Nov. 2018].
EMSA. (2018). *Sulphur Inspection Guidance*. [online] Available at: http://www.emsa.europa.eu/main/air-pollution/items.html?cid=149&id=2407 [Accessed 16 Oct. 2018].

European Commission. (2016). *Implementation of the Shipping MRV Regulation*. [online] Available at: https://ec.europa.eu/clima/sites/clima/files/transport/shipping/docs/working_paper_monitoring_plan_en.pdf [Accessed 24 Oct. 2018].

European Commission. (2018). *Monitoring, reporting and verification of EU ETS emissions - Climate Action - European Commission*. [online] Available at: https://ec.europa.eu/clima/policies/ets/monitoring_en [Accessed 19 Oct. 2018].

European Commission. (2018). *Reducing emissions from the shipping sector - Climate Action - European Commission*. [online] Available at: https://ec.europa.eu/clima/policies/transport/shipping_en [Accessed 19 Oct. 2018].

European Environment Agency. (2019). *Emission Factor Database*. [online] Available at: https://www.eea.europa.eu/publications/emep-eea-guidebook-2016/emission-factors-database [Accessed 22 Dec. 2018].

Fagerholt, K., Laporte, G. and Norstad, I. (2010). Reducing fuel emissions by optimizing speed on shipping routes. *Journal of the Operational Research Society*, [online] 61(3), pp.523-529. Available at: https://www.tandfonline.com/doi/full/10.1057/jors.2009.77 [Accessed 6 Dec. 2019].

Fagerholt, K., Gausel, N., Rakke, J. and Psaraftis, H. (2015). Maritime routing and speed optimization with emission control areas. *Transportation Research Part C: Emerging Technologies*, [online] 52, pp.57-73. Available at: https://www.sciencedirect.com/science/article/pii/S0968090X1400360X [Accessed 18 Oct. 2018].

Festus, D. and Samson, N. (2015). Effect of fluid density on ship hull resistance and powering. *International Journal of Engineering Research and General Science*, [online] 3(1), p.623. Available at: http://pnrsolution.org/Datacenter/Vol3/Issue1/80.pdf [Accessed 12 Nov. 2018].

Giorgiutti, Y., Rezende, F., Van, S., Monteiro, C. and Preterote, G. (2014). Impact of Fouling on Vessel's Energy Efficiency. In: *25o Congresso Nacional de Transporte Aquaviário, Construção Naval e Offshore*. [online] Rio de Janeiro: Bureau Veritas. Available at: https://www.veristar.com/portal/veristarinfo/files/sites/veristarinfo/web%20contents/bv-content/generalinfo/publications/bulletintechnique/Bulletin%20Technique%202014/Ship%20Energy%20Efficiency%20and%20Marine%20Renewable%20Energy/ship-energy-efficiency-and-marine-renewable-energy/documents/Impact%20of%20fouling%20on%20vessel%2527s.pdf [Accessed 11 Nov. 2018].

Global Development Research Center. (2018). *Sustainable Transportation*. [online] Available at: http://www.gdrc.org/uem/sustran/sustran.html [Accessed 17 Oct. 2018].

Górski, W., Abramowicz-Gerigk, T. and Burciu, Z. (2013). The influence of ship operational parameters on fuel consumption. *Maritime University of Szczecin*, [online] 36(108), pp.49-54. Available at:

https://www.researchgate.net/publication/312230471_The_influence_of_ship_operational_parameters_on_fuel_consumption [Accessed 14 Jan. 2019].

Graupe, D. (2007). *Principles of artificial neural networks*. 2nd ed. New Jersey: World Scientific.

Graves, A. (2014). *Supervised Sequence Labelling with Recurrent Neural Networks*. 1st ed. Berlin: Springer Berlin.

Green, J. (2018). *Why do we need new rules on shipping emissions? Well, 90 percent of global trade depends on ships.*. [online] Washington Post. Available at: https://www.washingtonpost.com/news/monkey-cage/wp/2018/04/17/why-do-we-need-new-rules-on-shipping-emissions-well-90-of-global-trade-depends-on-ships/?noredirect=on&utm_term=.c923bab7433e [Accessed 14 Dec. 2018].

Gusti, A. and Semin (2016). The Effect of Vessel Speed on Fuel Consumption and Exhaust Gas Emissions. *American Journal of Engineering and Applied Sciences*, [online] 9(4), pp.1046-1053. Available at: https://thescipub.com/pdf/10.3844/ajeassp.2016.1046.1053 [Accessed 31 Oct. 2018].

Gusti, A. and Semin, P. (2017). Speed Optimization Model for Reducing Fuel Consumption Based on Shipping Log Data. *International Journal of Marine and Environmental Sciences*, [online] 11(2), pp.359 - 362. Available at: https://waset.org/publications/10006404/speed-optimization-model-for-reducing-fuel-consumption-based-on-shipping-log-data [Accessed 20 Feb. 2019].

Hagan, M., Demuth, H., Beale, M. and De Jesús, O. (2016). *Neural network design*. 2nd ed. Oklahoma State University

Hagemeister, C. and Holmegaard Kristensen, H. (2011). *Environmental performance evaluation of RoPax ferries*. [online] Ship and Offshore. Available at: https://www.shipandoffshore.net/fileadmin/user upload/puplicationen/Shipandoffshore/2011-03/Environmental_performance-Specifics_of_RoPax_ferries.pdf [Accessed 16 Oct. 2018].

Hellio, C. (2009). *Advances in marine antifouling coatings and technologies*. Oxford: Woodhead, pp.161 - 1163.

IBM. (2018). *IBM Knowledge Center*. [online] Available at: https://www.ibm.com/support/knowledgecenter/fr/SS3RA7_15.0.0/com.ibm.spss.modeler.help/neuralnet_model.htm [Accessed 23 Dec. 2018].

ICCT. (2007). *Air Pollution and Greenhouse Gas Emissions from Ocean-going Ships: Impacts, Mitigation Options and Opportunities forManaging Growth*. [online] Available at: https://www.theicct.org/sites/default/files/publications/oceangoing_ships_2007.pdf [Accessed 15 Nov. 2018].

ICS Shipping. (2016). *European Union MRV Regulation*. [online] Available at: http://www.ics-shipping.org/docs/default-source/resources/ics-guidance-on-eu-mrv.pdf?sfvrsn=10 [Accessed 24 Oct. 2018].

IMO. (2009). *Second IMO GHG Study 2009*. [online] Available at: http://www.imo.org/en/OurWork/Environment/PollutionPrevention/AirPollution/Documents/SecondIMOGHGStudy2009.pdf [Accessed 22 Feb. 2019].

IMO. (2018). *Emission Control Areas (ECAs) designated under regulation 13 of MARPOL Annex VI (NOx emission control)*. [online] Available at: http://www.imo.org/en/OurWork/Environment/PollutionPrevention/AirPollution/Pages/Emission-Control-Areas-(ECAs)-designated-under-regulation-13-of-MARPOL-Annex-VI-(NOx-emission-control).aspx [Accessed 20 Oct. 2018].

IMO. (2018). *Energy efficiency and the reduction of GHG emissions from ships*. [online] Available at: http://www.imo.org/en/MediaCentre/HotTopics/GHG/Pages/default.aspx [Accessed 15 Oct. 2018].

IMO. (2018). *Energy Efficiency Measures*. [online] Available at: http://www.imo.org/en/ourwork/environment/pollutionprevention/airpollution/pages/technical-and-operational-measures.aspx [Accessed 26 Oct. 2018].

IMO. (2018). *IMO profile*. [online] Available at: https://business.un.org/en/entities/13 [Accessed 16 Oct. 2018].

IOBE (2014). The contribution of coastal shipping to the Greek economy: Performance and outlook. *Foundation for Economic and Industrial Research*. [online] Available at: http://iobe.gr/docs/research/en/RES_05_F_04112014_REP_EN.pdf [Accessed 22 Oct. 2018].

ISO. (2018). *ISO 14064-1:2006 - Greenhouse gases*. [online] Iso. Available at: https://www.iso.org/standard/38381.html [Accessed 21 Oct. 2018].

ITTC. (2014). *Analysis of Speed/Power Trial Data*. [online] Available at: https://ittc.info/media/4210/75-04-01-012.pdf [Accessed 5 Dec. 2018].

Kee, K., Lau Simon, B. and Yong Renco, K. (2018). Prediction of Ship Fuel Consumption and Speed Curve by Using Statistical Method. *Journal of Computer Science & Computational Mathematics*, [online] 8(2), pp.19-25. Available at: https://www.jcscm.net/fp/131.pdf [Accessed 20 Feb. 2019].

Keith, T. (2015). *Multiple regression and beyond*. 2nd ed. Routledge, Taylor and Francis.

Kim, M., Hizir, O., Turan, O., Day, S. and Incecik, A. (2017). Estimation of added resistance and ship speed loss in a seaway. *Ocean Engineering*, [online] 141, pp.465-476. Available at: https://www.sciencedirect.com/science/article/pii/S0029801817303530 [Accessed 5 Nov. 2018].

Kim, H., Chang, Y., Kim, K. and Kim, H. (2012). An epsilon-optimal algorithm considering greenhouse gas emissions for the management of a ship's bunker fuel. *Transportation Research Part D: Transport and Environment*, [online] 17(2), pp.97-103. Available at: https://www.sciencedirect.com/science/article/pii/S1361920911001337 [Accessed 18 Nov. 2018].

Koffi,, B., Cerutti, A., Duerr, M., Iancu., A., Kona, A. and Janssens-Maenhout, G. (2017). *CoM Default Emission Factors for the Member States of the European Union - Version 2017 - ecodp.common.ckan.site_title*. [online] European Commission. Available at: https://data.europa.eu/euodp/en/data/dataset/jrc-com-ef-comw-ef-2017 [Accessed 22 Feb. 2019].

Jang, J., Choi, S., Ahn, S., Kim, B. and Seo, J. (2014). Experimental investigation of frictional resistance reduction with air layer on the hull bottom of a ship. *International Journal of Naval Architecture and Ocean Engineering*, [online] 6(2), pp.363-379. Available at: https://www.sciencedirect.com/science/article/pii/S2092678216303077 [Accessed 9 Nov. 2018].

Lee,, J., Yoo, S., Choi, S., Kim, H., Hong, C. and Seo, J. (2014). Development and Application of Trim Optimization and Parametric Study Using an Evaluation System (SoLuTion) Based on the RANS for Improvement of EEOI. *Proceedings of the International Conference on Ocean, Offshore and Arctic Engineering.*, [online] 2. Available at: http://proceedings.asmedigitalcollection.asme.org/proceeding.aspx?articleid=1911534 [Accessed 18 Jan. 2019].

Lewis, E. (1988). *Principles of naval architecture*. Society of Naval Architects and Marine Engineers.

Lu, R., Turan, O. and Boulougouris, E. (2013). Voyage optimization: Prediction of ship specific fuel consumption for energy efficient shipping. *Low Carbon Shipping Conference*. [online] Available at: https://pdfs.semanticscholar.org/76b2/045bc6a3b96db02c5356f1b6c6efd7f5565e.pdf [Accessed 25 Oct. 2018].

Lundh, M., Garcia-Gabin, W., Tervo, K. and Lindkvist, R. (2016). Estimation and Optimization of Vessel Fuel Consumption. *IFAC-PapersOnLine*, [online] 49(23), pp.394-399. Available at: http://srv.uib.es/public/CAMS2016/media/files/0037.pdf [Accessed 3 Dec. 2018].

Magnussen, A. (2017). *Rational calculation of sea margin*. Ph.D. Norwegian University of Science and Technology.

Mannheim, D. (2017). *Application of AIS Data in Vessel Performance Analysis*. Master Thesis. Technical University of Denmark.

Maloni, M., Paul, J. and Gligor, D. (2013). Slow steaming impacts on ocean carriers and shippers. *Maritime Economics & Logistics*, [online] 15(2), pp.151-171. Available at: https://link.springer.com/article/10.1057/mel.2013.2 [Accessed 14 Oct. 2018].

Mander, S. (2017). Slow steaming and a new dawn for wind propulsion: A multi-level analysis of two low carbon shipping transitions. *Marine Policy*, [online] 75, pp.210-216. Available at: https://www.sciencedirect.com/science/article/pii/S0308597X16301300 [Accessed 16 Feb. 2019].

Marine Insight. (2017). *What is Nitrogen Oxides or NOx air pollution from Ships?*. [online] Available at: https://www.marineinsight.com/maritime-law/what-is-nitrogen-oxides-or-nox-air-pollution-from-ships [Accessed 19 Oct. 2018].

Marmer, E. and Langmann, B. (2005). Impact of ship emissions on the Mediterranean summertime pollution and climate: A regional model study. *Atmospheric Environment*, [online] 39(26), pp.4659-4669. Available at: https://pure.mpg.de/pubman/faces/ViewItemFullPage.jsp?itemId=item_994862_1 [Accessed 23 Oct. 2018].

Mersin, K., Alkan, G. and Mısırlıoğlu, T. (2017). A new method for calculating fuel consumption and displacement of a ship in maritime transport. *Cogent Engineering*, [online] 4(1). Available at: https://www.tandfonline.com/doi/pdf/10.1080/23311916.2017.1415107?needAccess=true [Accessed 5 Nov. 2018].

Moustafa, M., Yehia, W. and Hussein, A. (2015). Energy Efficient Operation of Bulk Carriers by Trim Optimization. *NAV 2015 18th International Conference on Ships and Shipping Research*.

Nayak, N. and Lakshminarayanan, P. (2013). *Critical component wear in heavy duty engines*. Hoboken, N.J.: Wiley.

Notteboom, T. (2010). The impact of low sulphur fuel requirements in shipping on the competitiveness of roro shipping in Northern Europe. *WMU Journal of Maritime Affairs*, [online] 10(1), pp.63-95. Available at: https://link.springer.com/article/10.1007/s13437-010-0001-7 [Accessed 27 Oct. 2018].

NPL. (2018). *Physical properties of sea water 2.7.9*. [online] Available at: http://www.kayelaby.npl.co.uk/general_physics/2_7/2_7_9.html [Accessed 13 Nov. 2018].

Nwaoha, T., Ombor, G. and Okwu, M. (2016). A combined algorithm approach to fuel consumption rate analysis and prediction of sea-worthy diesel engine-powered marine vessels. *Proceedings of the Institution of Mechanical Engineers, Part M: Journal of Engineering for the Maritime Environment*, [online] 231(2), pp.542-554. Available at: http://journals.sagepub.com/doi/abs/10.1177/1475090216663946 [Accessed 16 Oct. 2018].

OECD. (2018). *Decarbonising Maritime Transport*. [online] Available at: https://www.itf-oecd.org/decarbonising-maritime-transport [Accessed 20 Dec. 2018].

Oleksiy, B., Fukuda, T., Yoo, D. and Tanizawa, K. (2013). Development of Diesel Engine Simulator for Use with Self-Propulsion Ship Model. *Marine Engineering*, 48(5), pp.684-691.

Osborne, J. and Waters, E. (2002). Four Assumptions Of Multiple Regression That Researchers Should Always Test. *Practical Assessment, Research and Evaluation*, [online] 8(1), pp.1-5. Available at: https://pareonline.net/getvn.asp?v=8&n=2 [Accessed 16 Feb. 2019].

Pacetti, M. (2012). *The sustainable city VII*. Southampton: WIT.

Pedersen, B. and Larsen, J. (2009). Prediction of Full-Scale Propulsion Power using Artificial Neural Networks. In: *COMPIT '09: 8th International Conference on Computer and IT Applications in the Maritime Industries*. [online] Budapest, pp.537 - 550. Available at: https://pdfs.semanticscholar.org/8204/af25b322f673c918fce41ea9859be101199a.pdf [Accessed 11 Dec. 2018].

Petersen, J., Winther, O. and Jacobsen, D. (2012). A Machine-Learning Approach to Predict Main Energy Consumption under Realistic Operational Conditions. *Ship Technology Research*, [online] 59(1), pp.64-72. Available at: https://www.tandfonline.com/doi/abs/10.1179/str.2012.59.1.007 [Accessed 12 Feb. 2019].

Prpić-Oršić, J., Vettor, R., Faltinsen, O. and Guedes Soares, C. (2016). The influence of route choice and operating conditions on fuel consumption and CO2 emission of ships. *Journal of Marine Science and Technology*, [online] 21(3), pp.434-457. Available at: https://brage.bibsys.no/xmlui/bitstream/handle/11250/2469467/The+influence+of+route+choice+and+operating+conditions+on+fuel+consumption+and+CO2+emission+of+ships.pdf?sequence=2 [Accessed 4 Nov. 2018].

Raunek (2017). *What are Ro-Ro Ships?*. [online] Marine Insight. Available at: https://www.marineinsight.com/types-of-ships/what-are-ro-ro-ships/ [Accessed 19 Oct. 2018].

Roh, M. and Lee, K. (2017). *Computational ship design*. 1st ed. Springer, p.54.

Saraçoğlu, H., Deniz, C. and Kılıç, A. (2013). An Investigation on the Effects of Ship Sourced Emissions in Izmir Port, Turkey. *The Scientific World Journal*, [online] 2013, pp.1-8. Available at: https://www.hindawi.com/journals/tswj/2013/218324/ [Accessed 9 Jan. 2019].

Sharma, A. (2017). *Understanding Activation Functions in Neural Networks*. [online] Medium. Available at: https://medium.com/the-theory-of-everything/understanding-activation-functions-in-neural-networks-9491262884e0 [Accessed 21 Feb. 2019].

Shortsea. (2017). *Shipping emissions: lessons learned from the aviation industry | EENMA*. [online] Available at: https://www.shortsea.gr/shipping-emissions-lessons-learned-from-the-aviation-industry/ [Accessed 14 Oct. 2018].

SINTEF. (2018). *ShipX - SINTEF*. [online] Available at: https://www.sintef.no/en/software/shipx/ [Accessed 12 Dec. 2018].

Stevens, L., Sys, C., Vanelslander, T. and van Hassel, E. (2015). Is new emission legislation stimulating the implementation of sustainable and energy-efficient maritime technologies?. *Research in Transportation Business & Management*, [online] 17, pp.14-25. Available at: https://www.sciencedirect.com/science/article/pii/S2210539515000541 [Accessed 16 Oct. 2018].

Talley, W. (2012). *The Blackwell companion to maritime economics*. Chichester [England]: Wiley-Blackwell, p.385.

Tzannatos, E. and Stournaras, L. (2014). EEDI analysis of Ro-Pax and passenger ships in Greece. *Maritime Policy & Management*, [online] pp.1-12. Available at: https://www-tandfonline-com.plymouth.idm.oclc.org/doi/full/10.1080/03088839.2014.905722?scroll=top&needAccess=true [Accessed 16 Oct. 2018].

Tillig, F., Ringsberg, J., Mao, W. and Ramne, B. (2018). Analysis of uncertainties in the prediction of ships' fuel consumption – from early design to operation conditions. *Ships and Offshore Structures*, [online] 13(sup1), pp.13-24. Available at: https://www.tandfonline.com/doi/abs/10.1080/17445302.2018.1425519 [Accessed 29 Oct. 2018].

Townsin, R. (2003). The Ship Hull Fouling Penalty. *Biofouling*, [online] 19(sup1), pp.9-15. Available at: https://doi.org/10.1080/0892701031000088535 [Accessed 10 Nov. 2018].

Wan, Z., el Makhloufi, A., Chen, Y. and Tang, J. (2018). Decarbonizing the international shipping industry: Solutions and policy recommendations. *Marine Pollution Bulletin*, [online] 126, pp.428-435. Available at: https://www.sciencedirect.com/science/article/pii/S0025326X17310214 [Accessed 20 Oct. 2018].

Wang, S., Ji, B., Zhao, J., Liu, W. and Xu, T. (2017). Predicting ship fuel consumption based on LASSO regression. *Transportation Research Part D: Transport and Environment*. [online] Available at: https://www.sciencedirect.com/science/article/pii/S1361920917302109 [Accessed 17 Feb. 2018].

Wartsila. (2018). *Learning Center*. [online] Available at: https://www.wartsila.com/services/learning-center/ [Accessed 3 Dec. 2018].

Wartsila. (2018). *Ship resistance*. [online] Available at: https://www.wartsila.com/encyclopedia/term/ship-resistance [Accessed 25 Nov. 2018].

Wartsila. (2015) *White Papers*. [online] Improving Engine Fuel and Operational efficiency. (2015). Available at: https://cdn.wartsila.com/docs/default-source/services-documents/white-papers/wartsila-bwp---improving-engine-fuel-and-operational-efficiency.pdf?sfvrsn=b1fcc345_8 [Accessed 13 Jan. 2019].

Weintrit, A. and Neuman, T. (2013). *Marine Navigation and Safety of Sea Transportation*. Boca Raton, FL: Taylor and Francis, p.250.

Weintrit, A. and Neumann, T. (2017). *Safety of sea transportation*. 1st ed. Gdynia: Taylor and Francis, pp.72-74.

Woud, H. and Stapersm, D. (2002). *Design of Propulsion and Electric Power Generation Systems*. London: IMarEST Publication.

Yuan, J. and Nian, V. (2018). Ship Energy Consumption Prediction with Gaussian Process Metamodel. *Energy Procedia*, [online] 152, pp.655-660. Available at: http://The 15th International Symposium on District Heating and Cooling Ship Energy Consumption Prediction with Gaussian Process Metamodel Metamodel [Accessed 16 Nov. 2018].

Zis, T. and Psaraftis, H. (2017). The implications of the new sulphur limits on the European Ro-Ro sector. *Transportation Research Part D: Transport and Environment*, [online] 52, pp.185-201. Available at: https://www.sciencedirect.com/science/article/pii/S1361920916308203 [Accessed 16 Oct. 2018

A. Ship's Total Resistance Equations

Hull Resistance in calm waters

The ship's resistance is given by the ITTC – 57 (2014) formula below:

$$\boldsymbol{R = \frac{1}{2}\,\rho\, C_t\, V^2\, S} \qquad \textbf{(A.1)}$$

where:
$R = Total\ Resistance$
$C = Total\ Resistance\ coefficient$
$V = speed$
$S = wetted\ surface$
$\rho = fluid\ density$

Therefore, Molland (2011) concluded that the total resistance in calm waters is estimated as the sum of other resistances:

$$\boldsymbol{R_{total} = R_F\,(1 + k_1) + R_{APP} + R_W + R_B + R_{TR} + R_A} \qquad \textbf{(A.2)}$$

where:
$R_{total} = Total\ Resistance$
$R_F = Frictional\ Resistance$
$1 + k_1 = factor\ describing\ the\ viscous\ resistance\ in\ relation\ to\ R_F$
$R_{APP} = Appendage\ Resistance$
$R_W = Wave\ making\ and\ Wave\ breaking\ Resistance$
$R_B = Additional\ Resistance\ of\ bulbous\ bow\ in\ the\ water\ surface$
$R_{TR} = Additional\ pressure\ resistance\ of\ the\ immersed\ transom\ stern$
$R_A = model\ ship\ correlation\ resistance$

At this point, it should be noted that Frictional Resistance (R_F) is dependent on Reynold Number (R_e) Reynold Number, which is expressed as a function of water's density and viscosity (Appendix 1). Both are related to fluid's temperature *(T)* and thus variations are observed in the values of R_F and R_e. For this reason, corrections are applied to the model and the resistance is calculated for $T = 15°C$ (Molland, 2011). The frictional resistance can be estimated by the following equation provided by the ITTC – 57 (2014):

$$\boldsymbol{R_F = \frac{1}{2}\,\rho V^2\, S C_F} \qquad \textbf{(A.3)}$$

The $1 + k_1$ can be found by the following formula:

$$\mathbf{1 + k_1 \ = c_{13}\{0.93 + c_{12}\,(B/L_R)^{0.92497}\,(0.95 - \ C_P)^{-0.521448}\,(1 - C_P \ + 0.0225\,lcb)^{0.6906}\}} \qquad \textbf{(A. 4)}$$

where:

$$\mathbf{c_{13} \ = 1 + 0.003\ C_{Stern}} \qquad \textbf{(A.5)}$$

For afterbody forms:
V – shaped sections, then: $C_{Stern} = -10$
Normal sections shape, then $C_{Stern} = 0$
U – shaped with Hogner stern, then $C_{Stern} = +10$

$c_{12} = (T/L)^{0.2228446}$ when $T/L > 0.05$

$c_{12} = 48.20\,(T/L - 0.02)^{2.078} + 0.479948$ when $0.02 < T/L < 0.05$

$c_{12} = 0.479948$ when $T/L < 0.02$

$L = waterline\ length$
$T = average\ moulded\ draught$

$S =$
$L\,(2T + B)\sqrt{C_M}\,(0.453 + 0.4425C_B - 0.2862C_M - 0.003467\,B/T + 0.3696C_{WP}) + 2.38\,A_{BT}/C_B -$
Wetted surface of the hull

$C_M \ = midship\ section\ coefficient$
$C_B \ = block\ coefficient$

$C_P \ = prismatic\ coefficient$

- The Frictional Resistance Coefficient is provided by the following equation:

$$\mathbf{C_F \ = \frac{0.075}{(log_{10}\,R_e - 2)^2}} \qquad \textbf{(A.6)}$$

- Reynold's Number formula:

$$\mathbf{R_e \ = \rho v l/\mu} \qquad \textbf{(A.7)}$$

- Appendage Resistance can by found by the following formula:

$$\mathbf{R_{APP} \ = \frac{1}{2}\,\rho V^2\,S_{APP}\ (1 + k_2\ )_{eq}\,C_F} \qquad \textbf{(A.8)}$$

where:
$S_{APP} \ = wetted\ surface\ of\ appendages$

$1 + k_2 \ = appendage\ resistance\ factor$

For Stabilizer fins the factor takes the value: $1 + k_2 \ = 2.8$

• Bow thruster resistance can be found by the following equation:

$$\boldsymbol{R_{BTO}} = \boldsymbol{\rho V^2 \pi d^2 C_{BTO}} \quad \textbf{(A.9)}$$

where:

d = the tunnel diameter

C_{BTO} takes value between 0.003 and 0.012

• The wave making and wave breaking resistance is provided by the following formula:

$$\boldsymbol{R_W} = \boldsymbol{c_1 c_2 c_3 \nabla} \ \rho g \ \exp\{\boldsymbol{m_1 F_n^d} + \boldsymbol{m_2} \cos(\boldsymbol{\lambda F_n^{-2}})\} \quad \textbf{(A.10)}$$

• The Additional pressure of bulbous bow is given by the equation below:

$$\boldsymbol{R_{TR}} = \boldsymbol{0.11 \exp\left(-3P_B^{-2}\right) F_{ni}^3 A_{BT}^{1.5} \rho g / (1 + F_{ni}^2)} \quad \textbf{(A.11)}$$

while the additional pressure resistance of immersed transom stern is given by:

$$\boldsymbol{R_{TR}} = \frac{1}{2} \boldsymbol{\rho V^2 A_T c_6} \quad \textbf{(A.12)}$$

c_6 is dependent on F_{nT}

$c_6 = 0.2\ (1 - F_{nT})$ when $F_{nT} < 5$
$c_6 = 0$ when $F_{nT} \geq 5$

• Froude number based on immersed transom stern is provided by the following equation:

$$\boldsymbol{F_{nT}} = \boldsymbol{V / \sqrt{2g\, A_T\, (B + BC_{WP})}} \quad \textbf{(A.13)}$$

• The model ship correlation resistance is provided by the formula below:

$$\boldsymbol{R_A} = \frac{1}{2} \boldsymbol{\rho V^2 S C_A} \quad \textbf{(A.14)}$$

$$C_A = 0.006\ (L + 100)^{-0.16} - 0.00205 + 0.003 \sqrt{\frac{L}{7.5}}\ C_B^4\ c_2 (0.04 - c_4)$$

with
$c_4 = T_F / L$ when $T_F / L \leq 0.04$
$c_4 = 0.04$ when $T_F / L > 0.04$

• Total Resistance for the reference water is given by:

$$\boldsymbol{R_{TO}} = \frac{\mathbf{1}}{\mathbf{2}}\,\boldsymbol{\rho_{TO} V^2\, SC_{TO}} \quad \textbf{(A.15)}$$

Total Resistance

All equations in this chapter are provided by the ITTC (2014)

Total Resistance $\boldsymbol{R_T}$ is provided by the following equation:

$$\boldsymbol{\Delta R = R_{AW} + R_{AA} + R_{AS}}, \quad \textbf{(A.16)}$$

where:
$R_{AW} = Added\ Resistance\ due\ to\ Waves$
$R_{AA} = Added\ Resistance\ due\ to\ Wind$
$R_{As} = Added\ Resistance\ due\ to\ Sea$

Added Wave Resistance $\mathbf{R_{AW}}$

ISO (2018) standards introduced two empirical methods, STAWAVE 1 and STAWAVE 2, for the estimation of the mean added wave resistance (R_{AWL}).

STAWAVE 1 method is applied to larger vessels and it is used in order to estimate head waves taking into account that the heave and the pitch are insignificant (ITTC, 2014). This method is used when the significant wave height should comply with the following restriction:

$$H_{1/3} \leq 2.25\sqrt{LBP/100}$$

STAWAVE 2 describes the $\boldsymbol{R_{AWL}}$ in crested irregular waves in relation to ship's speed, wave's characteristics and combines both the wave reflection resistance $\boldsymbol{R_{AWRL}}$ and the induced motion resistance $\boldsymbol{R_{AWML}}$ in regular waves (Magnussen, 2017). The mean added resistance is given by the following formula:

$$\boldsymbol{R_{AWL} = 2\int_0^\infty \frac{R_{wave}(\omega;V_S)}{\zeta_A^2}\, S_\eta(\omega)\, d\omega} \quad \textbf{(A.17)}$$

where:
$R_{AWL} = Mean\ Added\ Resistance\ due\ to\ waves\ (N)$
$R_{wave} = Mean\ Added\ Resistande\ due\ to\ regular\ waves\ (N)$
$S_\eta = Frequency\ spectrum\ (m^3 s)$
$V_S = Vessel\ Speed\ through\ the\ water\ (m/s)$
$\zeta_A = Wave\ amplitude\ (m)$
$\omega = Circular\ frequency\ of\ regular\ waves\ (rad/s)$

This formula is applied when the following restrictions are met:

$75\ (m) < L_{pp} < 350\ (m)$ (if the length between perpendiculars is more than 75m and less than 350m)

1. $4.0 < \frac{L_{pp}}{B} < 9.0$ (if the ratio of the length between perpendiculars and vessel's breadth is more than 4.0 and less than 9,0)

2. $2.2 < \frac{B}{T} < 5.5$ (if the ratio of the vessel's breadth and draught is more than 2.2 and less than 9.0)
3. $0.10 < F_r < 0.30$ (when the Froude Nr. (F_r) takes values between 0.10 and 0.30)
4. $0.50 < C_B < 0.90$ (when the block coefficient (C_B) takes values between 0.50 and 0.90
5. $-45° < a_w < 45°$ (when the wave direction is within 0° to $\pm$ 45° from the bow

• The mean added resistance increase due to regular wave:

$$\boldsymbol{R_{wave} = R_{AWRL} + R_{AWML}} \quad \textbf{(A.18)}$$

• Resistance increase due to wave reflection is given by the following equation:

$$\boldsymbol{R_{AWRL} = \frac{1}{2}\rho g \zeta_A^2 B a_1(\omega)} \quad \textbf{(A.19)}$$

where:

$\rho = water\ density\ (^{kg}/_{m^3})$
$g = gravity\ constant\ (g = 9.8\ ^{m}/_{s^2})$
$\zeta_A = wave\ amplitude\ (m)$
$B = Ship's\ breadth\ (m)$
$\omega = Circular\ frequency\ of\ regular\ waves\ (^{rad}/_{s})$
$C_B = block\ coefficient$
$T_M = midship\ draught\ (m)$
$k = wave\ number\ (^{rad}/_{m})$
$I_1 = modified\ Bessel\ function\ of\ the\ first\ kind\ of\ order\ 1$
$K_1 = modified\ Bessel\ function\ of\ the\ second\ kind\ of\ order\ 1$

Another way to estimate the added resistance due to waves and wind is through the Kwon (2008) formula as it connects the involuntary speed loss with the added resistance due to weather conditions (Molland, 2011). The Kwon formula is applied to all vessels except container ships and is given by the following formula:

$$\alpha \cdot \mu \frac{\Delta V}{V}\ 100\% \quad \textbf{(A.20)}$$

where:

$\alpha = correction\ coefficient\ for\ C_B$
$\mu = weather\ direction\ reduction\ coefficient$
$V_1 = Operating\ speed\ in\ calm\ waters\ (^{m}/_{s})$
$V_2 = Speed\ in\ specific\ weather\ conditions\ (^{m}/_{s}) - \ irregular\ waves\ and\ wind$
$\Delta V = Speed\ difference\ (m/s)$
$\Delta V = V_1 - V_2$
$\frac{\Delta V}{V} = Speed\ loss\ \%$

Added Resistance due to wind

The added resistance due to wind ($\boldsymbol{R_{AA}}$) can be found with the following equation:

$$\boldsymbol{R_{AA} = \frac{1}{2}\,\rho_{air} A_T C_{Dwind}\{(U_{wind} + V_w)^2 - V_C^2\}}, \quad \textbf{(A.21)}$$

where:
$R_{AA} = Added\ Resistance\ due\ to\ wind\ (N)$
$\rho_{air} = Air\ density$
$V_W = Wind\ velocity$
$C_D = Air\ Drag\ Coefficient$
$A_T = Ship's\ above\ waterline\ area$
$U_{wind} = Wind\ speed$
$V_c = Vessel's peed\ over\ ground$
At this point it should be stated that $\boldsymbol{\rho_{air}}$ will take the value 1.23 kg/m^3 . The wind speed $\boldsymbol{U_{wind}}$ will be provided by the Table that depicts the B.N expressed as wind direction and speed.
7.1.2.3 Added Resistance due to Roughness and Fouling

$$\boldsymbol{\Delta R_{F=}\ \frac{1}{2}\,\rho\, V^2\, S\, \Delta C_F}, \quad \textbf{(A.22)}$$

where:

$\boldsymbol{\Delta C_F}$ is the change in the frictional coefficient and its formula is provided by Towsin (2003):

$$\boldsymbol{\Delta C_{F=}\ 0.044\left[\frac{AHR^{\frac{1}{3}}}{L_{pp}} - 10\left(\frac{1}{Re_{Lpp}}\right)^{\frac{1}{3}}\right] + 0.000125}, \quad \textbf{(A.23)}$$

where:
$AHR = Average\ hull\ Roughness$
$R_e = Reynold\ Number$
$L_{PP} = Length\ Between\ Perpendiculars$

Added resistance due to seawater composition

The ISO (2015) provided the formula of the resistance increase due to seawater's composition and is estimated by:

$$\boldsymbol{R_{AS} = R_{TO}\left(\frac{\rho_s}{\rho_{so}} - 1\right) - R_F\left(\frac{C_{FO}}{C_F} - 1\right)}, \quad \textbf{(A.24)}$$

where:

$R_{AS} = Added\ Resistance\ due\ to\ seawater$
$R_{TO} = Resistance\ for\ the\ reference\ water$
$R_F = Frictional\ Resistance\ for\ the\ actual\ water$
$C_F = Frictional\ Resistance\ coefficient\ for\ the\ actual\ water$
$C_{TO} = Resistance\ coeficient\ for\ the\ reference\ water$
$\rho_s = density\ for\ the\ actual\ water$
$\rho_{TO} = density\ for\ the\ actual\ wate\boldsymbol{r}$

However, these properties are relative to location and season. Since the vessel under study is performing on a specific itinerary, variations in the temperature, viscosity and density are minor. Nevertheless, in our model a difference of $\pm 10° C$ in temperature will be applied due to season weather conditions (Magnussen, 2017). Therefore, the model will be corrected and the additional resistance will be estimated based on the typical seawater temperature ($T = 15° C$) and density $\rho = 1{,}026\ kg/m^3$.

B. Ship Power Train

In this subsection all the necessary formulas in order to estimate the engine's horsepowers are provided according to ICCT (2014)

- Effective Horsepower (EHP):

$$\boldsymbol{P_E = R_T\, x\, V,} \qquad \textbf{(B.1)}$$

where :
$R_T = the\ total\ hull\ resistance$
$V = the\ ship's\ speed$

- Quasi - Propulsive Coefficient (QPC):

$$\boldsymbol{QPC = {P_E}/{P_D}\ ,} \qquad \textbf{(B.2)}$$

where:
$P_E = EHP$
$P_D = DHP$

or through the Emerson formula:

$$\boldsymbol{QPC = 0.84 - \frac{N - LBP^{0.5}}{10000}\ ,} \qquad \textbf{(B.3)}$$

where:
$N = propeller\ rpm$
$LBP = length\ between\ perpendiculars$

C. Activation Functions

1. Binary Activation Function or Step Function

The neuron is activated if the following restriction is met:

$$f(x) = \begin{cases} 0 \; for \; x < 0 \\ 1 \; for \; x \geq 0 \end{cases} \quad \textbf{(C.1)}$$

It is understood that the neuron is activated if the total value of its output is ≥0 (threshold) while it is not fired when the value is < 0. The plot of the activation function is given below:

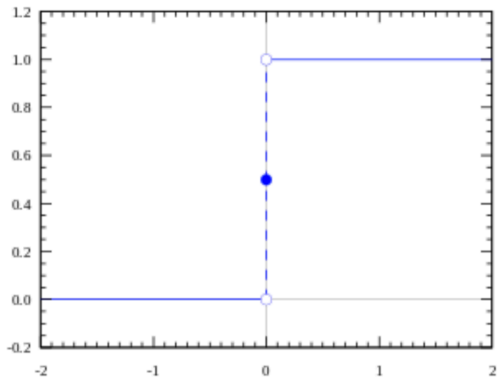

Figure 22: Binary Activation Function Plot (source: Sharma,2017)

2. Linear Activation Function

$$f(x) = cx \quad \textbf{(C.2)}$$

The plot of the activation function is given below:

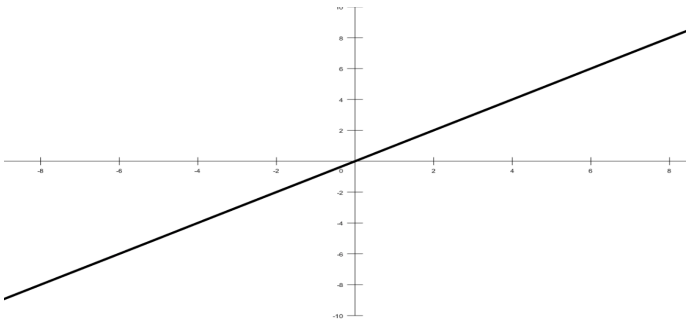

Figure 23: Linear Activation Function Plot (source: Sharma,2017)

3. Logistic Sigmoid Activation Function

Sigmoid is a differentiable non-linear activation function and its output takes values between 1 and 0.

$$\boldsymbol{f(x) = \sigma(x) = \frac{1}{(1+e^{-x})}} \quad \textbf{(C.3)}$$

The plot of the Logistic Sigmoid Activation Function is provided below:

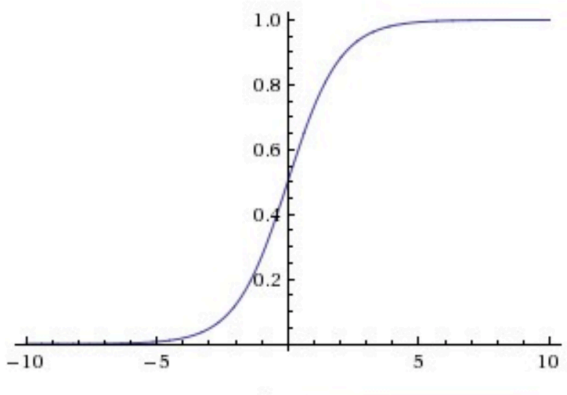

Figure 24: Logistic Sigmoid Activation Function Plot (source: Sharma, 2017)

4. Hyperbolic Tangent (tanh) Activation Function

It has similar characteristics to sigmoid while its output takes values between -1 and 1.

$$\boldsymbol{f(x) = \tanh(x)\ \frac{(e^{x}-e^{x})}{(e^{x}+e^{-x})}} \quad \textbf{(C.4)}$$

The plot of the aforementioned activation function is given below:

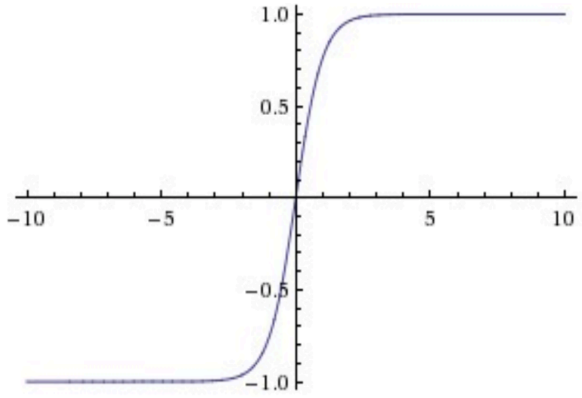

Figure 25: Hyperbolic Tangent Activation Function Plot (source: Sharma, 2017)

5. RELU (Rectified Linear Unit) Activation Function

$$f(x) = \begin{cases} 0 \; for \; x < 0 \\ x \; for \; x \geq 0 \end{cases} \quad \textbf{(C.5)}$$

The plot of the aforementioned function is given below

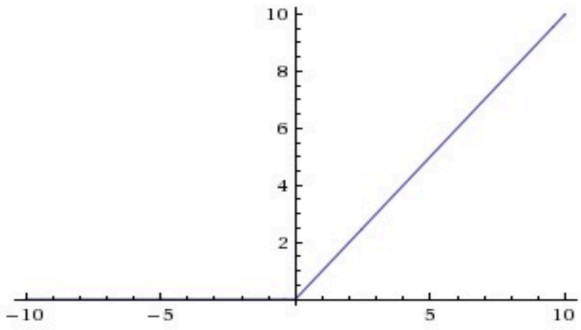

Figure 26: RELU Activation Function Plot (source: Sharma, 2017)

D. ANNs Architecture

I. The FFNN's architecture under the Scenario1 is presented below:

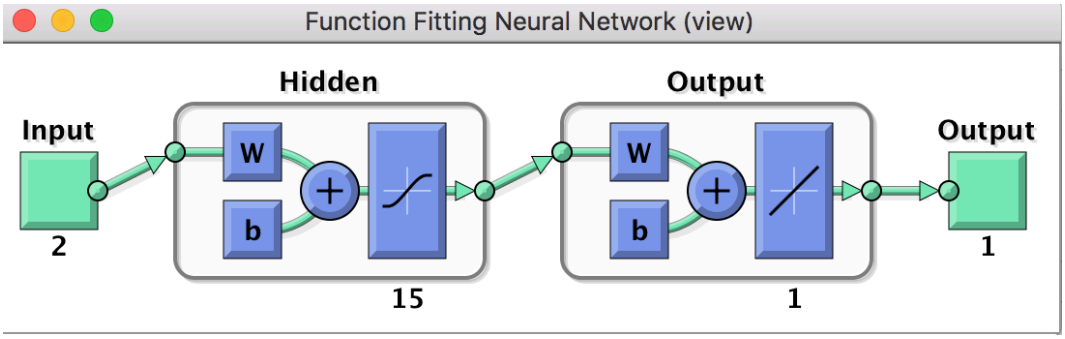

Figure 27: 1st Scenario FFNN model under MATLAB Neural Fitting (nftool) (source: author)

II. The FFNN's architecture under the Scenario 2 is presented below:

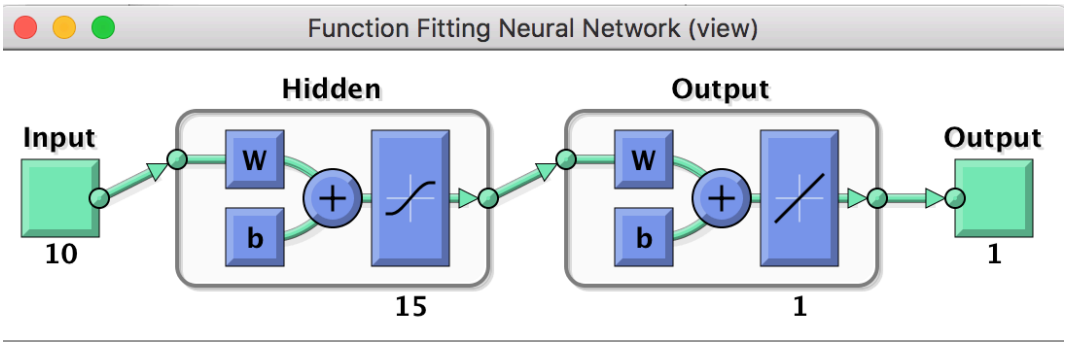

Figure 28: 2nd Scenario FFNN model under MATLAB Neural Fitting (nftool) (source: author)

III. The FFNN's architecture under the Scenario 3 is presented below:

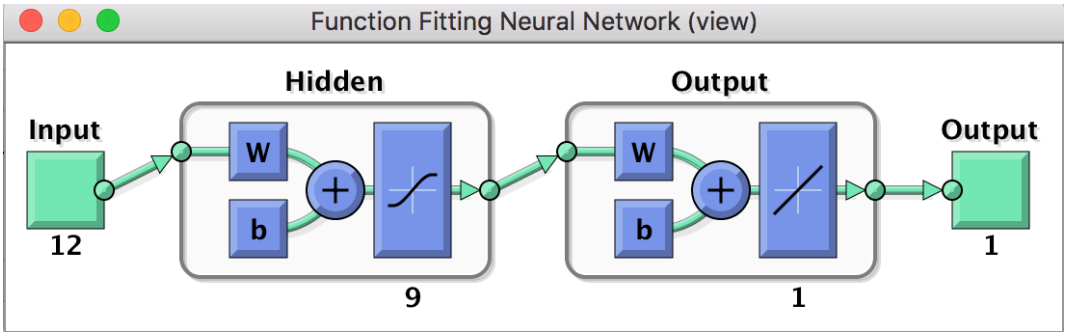

Figure 29: 3rd Scenario FFNN model under MATLAB Neural Fitting (nftool) (source: author)

E. Multiple Regression Analysis Outcomes

The outcomes from the Regression Analysis Outcomes and more precisely the coefficients and the variables used in the three regression models are illustrated in table below:

Table 11: Regression Analysis Outcomes (stepwise method)

Coefficients (stepwise method)								
Model		Unstandardized Coefficients		Standardized Coefficients	t	Sig.	Collinearity Statistics	
		B	Std. Error	Beta			Tolerance	VIF
1	(Constant)	55.217	.187		295.707	.000		
	Zscore(ME_LSFO_fc)	2.289	.188	.838	12.166	.000	1.000	1.000
2	(Constant)	55.217	.154		358.780	.000		
	Zscore(ME_LSFO_fc)	2.042	.161	.747	12.650	.000	.923	1.083
	Zscore(avg_speed)	-.895	.161	-.327	-5.545	.000	.923	1.083
3	(Constant)	55.217	.144		384.154	.000		
	Zscore(ME_LSFO_fc)	1.943	.154	.711	12.628	.000	.886	1.129
	Zscore(avg_speed)	-.981	.153	-.359	-6.404	.000	.895	1.118
	Zscore(pax)	.473	.149	.173	3.175	.002	.945	1.059

(source: author)